Computational Modeling and Experimental Studies on NO_x Reduction Under Pulverized Coal Combustion Conditions

Final Technical Report
February 1, 1995 - May 31, 1998

Subha K. Kumpaty
Kannikeswaran Subramanian
Victor P. Nokku
Tyrus L. Hodges
Adel Hassouneh
Ansumana Darboe
Sravan K. Kumpati

Rust College
Holly Springs, MS 38635

Report Issue Date: May 1, 1998

Submitted to:

U.S. Department of Energy
Pittsburgh Energy Technology Center
P.O. Box 10940
Pittsburgh, PA 15236-0940

Work Performed Under the Contract DE-FG22-95PC94254--12

U.S. DOE PATENT CLEARANCE
NOT REQUIRED
PRIOR TO PUBLICATION OF
THIS REPORT

DISCLAIMER

This report was prepared as an account of work sponsored by an agency of the United States Government. Neither the United States Government nor any agency thereof, nor any of their employees, makes any warranty, express or implied, or assumes any legal liability or responsibility for the accuracy, completeness, or usefulness of any information, apparatus, product, or process disclosed, or represents that its use would not infringe privately owned rights. Reference herein to any specific commercial product, process, or service by trade name, trademark, manufacturer, or otherwise does not necessarily constitute or imply its endorsement, recommendation, or favoring by the United States Government or any agency thereof. The views and opinions of authors expressed herein do not necessarily state or reflect those of the United States Government or any agency thereof.

ACKNOWLEDGMENTS

The principal investigator, Dr. Subha K. Kumpaty and the institution, Rust College, Holly Springs, Mississippi would like to thank the federal agency, United States Department of Energy for the opportunity to involve in research related to NO_x control under this grant instrument No. DE-FG22-95PC94254. We have several people to thank who contributed greatly in making this work possible.

To the Secretary of Energy, Honorable Hazel O'Leary and the Office of Economic Impact and Diversity crew: Ms. Corlis S. Moody and Ms. Annie Whatley for their special interest in assisting small colleges and universities like ours,

To the DOE representative, Mr. Casters Foster who encouraged us in grant seeking by his personal visit to the campus,

To the Contracting Officer, Mr. William R. Mundorf and the grant administration specialist, Ms. Mary-Beth Pearse, for their excellent cooperation throughout the grant period,

To the Contracting officer's Technical Representative (COTR), Dr. Lori D. Gould and Mr. James Ekmann for their technical guidance in the early stages of the experimental plan, and to the subsequent COTRs Dr. Udaya Rao and Dr. Mildred Perry for their technical support,

To Sandia National Laboratories for making CHEMKIN package available for use in this research and in particular to Ms. Fran Rupley for the initial technical help in its use,

To Mr. Nick Ridge, Vice President, Environmental Protection Systems, Memphis, TN for his partnership in our efforts to meet environmental regulations,

To Mr. Kannikeswaran Subramanian for his expert guidance in experimental,

To all in the Rust College family who cheered us through thick and thin and steered us to completion,

and to God,

we gratefully acknowledge our sincere thanks.

TABLE OF CONTENTS

LIST OF TABLES

LIST OF FIGURES

Chapter I

INTRODUCTION AND LITERATURE SURVEY

This work was an attempt to develop a NO_x reduction technology that provides important data for industrial pollution control. The major objective of this work was to find the most achievable control technology which is called for by the CAAA 1991 hazardous organic National Emission Standards for hazardous air pollutants, thereby help the industry in reducing emissions significantly and contribute to the society in large which is plagued by pollution problems, the most threatening one being NO_x. In achieving this objective, this research work contributed directly toward 1) expanding the current Rust College research pertaining to the char and nitrogen reaction mechanisms in combustion environments in order to make a contribution to DOE/FE intent and current needs in the form of advanced high efficiency pollution emissions control, 2) improving the scope of research performed by the group by establishing an experimental base, 3) expanding the breadth of undergraduate education at Rust College by students working in the group and 4) enhancing the Rust College linkage with the private sector fossil energy community. Specifically a team effort involving faculty members and students expanded present research activities in the area of NO_x reduction in coal combustion. This team built on a foundation of work supported by the Faculty/Student Exploratory Grant #DE-FG22-MT92022. This research opportunity enhanced the Rust College participation in fossil research and contributed towards the HBCU faculty and student development.

The major area of concentration of the research was NO_x reduction during pulverized coal combustion using reburning technique. Historically, the reburning chemistry has been

of recent origin with an immense potential for further research and understanding. A scientific understanding is needed of the interactions of the different gaseous reburning fuels as well as the effects of surface catalyzed reactions (using calcium associated compounds) in the nitrogen oxides emission control. This research work involved a strong experimental component as well as a strong computational modeling component. The research focussed on understanding the interactions of various chemical species and determining the key chemical reactions that affect the formation and destruction of NO_x. The research has a major impact on industrial pollution control by providing the important data related to the reduction of NO_x. This research contributes directly to DOE needs in terms of advanced high efficiency emissions control.

1.1 Introduction

Coal is a major contributor of the fossil fuel energy reserves. Though coal is surplus in availability and attractive in price, its combustion involves the production of pollutants. Therefore the utility of coal suffers a serious setback. One type of coal pollutant from coal combustion is NO_x (NO, NO_2, and N_2O), which is toxic and ozone depleting. High fuel nitrogen to NO_x conversion efficiency (40-60%), coupled with growing stringent regulations calls for advanced technologies.

The NO_x control technologies currently available are NO_x reduction during combustion (low NO_x burner, staged combustion) and post-combustion (selective and non-selective catalytic reduction). The control technologies, fuel staging (reburning) and non-selective catalytic reduction have been claimed to be individually effective in reducing NO_x.

The present NO_x emission control regulations have become much more stringent and hence modification in the existing technology or a combination of the two technologies is an absolute necessity. Part of this work was reduction of NO using hybrid technology of reburning and non-selective catalytic reduction.

In the recent past, fuel staging (reburning) has been found to be very effective in reducing NO_x. It was also identified that C, CH, CH_2 and other hydrocarbon radicals are responsible for NO_x reduction. Studies needed to be conducted with methane (CH_4) and acetylene (C_2H_2), as these gases are rich sources of carbon and hydrogen essentially creating a reducing atmosphere. The computational modeling of the nitric oxide reduction was studied, under the identical reburning conditions. A comparative study of the experimental and the computational modeling was the focal point of this work.

Hansen et al (1992) reported that CaS (which is reported to be formed as a result of reduction from $CaSO_4$) could be an active catalyst surface in reducing NO, and that CO_2 does not deactivate the active catalyst surface of CaS. In our study metered quantity of pure CaS was tested for its catalytic activity in methane reburning conditions at a stoichiometric ratio of 0.9. Since we expected calcium to aid in reducing NO_x by catalytic surface reduction and since calcium carbide by itself is a reducing agent, we chose to perform studies with CaS and CaC_2. We expected the synergetic NO_x reduction by hybridizing the catalytic surface reduction with these calcium compounds in methane reburning conditions.

Recent research work by Teng et al (1992), has shown that gasification of NO by lignite char is responsible for NO_x reduction mechanism. The effectiveness of lignite char was also studied under this grant instrument.

1.2 Scientific Discussion

The mechanism leading to NO_x emission, during coal combustion could be greatly understood, if a thorough knowledge on the coal nature, coal structure and coal combustion is known.

1.2.1 NO_x formation mechanism

NO_x formed by combustion is basically by three mechanisms namely thermal NO_x, prompt NO_x, and fuel NO_x (Bowman et al. 1991). Thermal NO_x formation was first postulated by Zeldovich. When any fuel is burned in air the heat of the reaction increases the degree of dissociation of molecular nitrogen and oxygen. Thermal NO_x is formed when these dissociated products produce NO by the well-known extended Zeldovich mechanism (Miller and Fisk, 1987).

$$N + O_2 \text{-----} NO + O \qquad \textbf{(R1)}$$

$$O + N_2 \text{-----} NO + N \qquad \textbf{(R2)}$$

Thermal NO_x is most pronounced in lean, high temperature flames with long residence times. From Fenimore studies (Fenimore, 1971), it is found that prompt NO_x is formed as a result of attack by the hydrocarbon fragments on the molecular nitrogen.

$$CH + N_2 \text{-----} HCN + N \qquad \textbf{(R3)}$$

$$CH + N_2 \text{-----} HCN + NH \qquad \textbf{(R4)}$$

The products of the above reactions react together forming prompt NO_x. The third principal source of NO_x in combustion systems is nitrogen, that is chemically bound in the fuel.

Scanning electron microscope (SEM) photographs of pulverized coal particles show drastic difference in surface area and roughness for particles of different coals (Haider, 1982). Also, surface porosity measured by absorption has been shown to be an important variable in reactivity (Seeker, 1979) and researchers have further classified coals as large pore and small pore coals. The complex molecular structures of coals have also been found to contain significant variations in basic structures as well as functional groups (Chen et al. 1982). In a recent research work by Helble et al. (1990), striking differences were noted among the various coals, which were traced to the differences in mineralogies of the plant fuels.

Although the total quantity of nitrogen present in the coal is small compared to the molecular nitrogen in the combustion air, the high conversion efficiency of fuel nitrogen to NO_x (15 - 40%), (Arthur Levy, 1982) makes fuel NO an important NO producing mechanism. It was found by Song et al. (1982) that volatilized nitrogen compounds accounted for a major fraction of NO_x produced from coal nitrogen, especially at high temperatures and low fuel oxygen equivalence ratios. The fuel NO_x producing mechanism is analyzed using CHEMKIN kinetic analysis package (Lutz et al. 1988) by Miller and Bowman (1989). It is shown that the majority of NO is reduced by radicals C, CH, CH_2 to HCN and amine radicals (NH_i). Also studies by Blair and Wendt (1981) have revealed that HCN and NH_3 are the two major nitrogen containing compounds. The amine radicals in turn, can be converted to N_2 or NO. The nitric oxide formed as a result of the above mechanisms is toxic, ozone depleting and contributes to photochemical smog. Hence, every effort to control NO_X

emission is crucial and vital.

1.2.2 NO_X emission control

The two major stages of NO_x emission control are 1) the combustion stage and 2) the post-combustion stage. The pre-combustion cleaning operations are not effective in removing fuel bound nitrogen. The major NO_x control strategies under combustion stage are

a) low NO_x burners such as cyclone boiler, tangentially fired boiler, and wall fired boilers in which the conversion of nitrogen to NO_x is retarded by delaying the mixing of fuel and air in the combustion zone,

b) air staging in which air ports are added in the furnace wall above the burners to create a fuel rich low NO_x combustion zone and

c) fuel staging (reburning), wherein a small amount of natural gas, or coal is injected above the normal combustion zone to form an oxygen deficient zone.

The significant NO_x control strategies under post-combustion are a) selective catalyst reduction (SCR) and b) non-selective catalyst reduction (NSCR).

The selective catalyst reduction works on the principle of selectively reducing NO_x using some catalyst. The selective catalytic reduction is frequently dismissed due to its extremely high capital and annualized "use cost". The non- selective catalytic reduction works on the principle of gas phase reaction of nitrogen based reagent, typically ammonia or urea. One of our objectives of this work was to use hybrid technology of fuel staging and non-selective catalytic reduction to effectively reduce NO.

1.2.2.1 Current reburning research projects

Reburning or fuel staged combustion is the name given to a NO_x reducing combustion

modification proposed by Wendt et al. (1973). Reburning is the intermediary stage between the primary zone and the burn-out zone in which fuel rich atmosphere is produced by injecting another fuel, there by creating reducing environment for NO_x reduction. In the primary zone, which is characterized by the stoichiometric ratio SR1, most of the fuel is consumed, and it is usually fuel lean. In the burn-out zone (characterized commonly by the stoichiometric ratio, SR3), enough additional air is sent to complete the combustion process. Since the coal has a high fuel nitrogen content and the first stage flame is fuel lean (promoting a high conversion of fuel nitrogen to NO) the concentration of NO_x at the exit of the first stage may be as high as 1000 ppm. However, other fixed nitrogen compounds such as HCN, NH_3 are minimal due to its lean stoichiometry. Reburning zone is characterized by the stoichiometric ratio, SR2, which is referred to frequently throughout this work.

Reductive powers of hydrocarbons in the conversion of NO_x to N_2 were first discovered and reported by Engel (1950) and Patry and Engel (1950). However the reburning concept accomplishing fifty percent NO_x removal was reported only in 1983, when Takahashi et al. (1983) reported results using natural gas as a reburning fuel. Mulholland and Lanier (1984) studied NO_x control by reburning in a firetube package boiler. Energy and Environment Research Corporation (Greene and Weaver, 1974; Overmoe et al. 1986), and U.S. Environmental Protection Agency (Mulholland and Hall. 1986) conducted NO_x research work on stationary combustion systems.

Coal was identified as the most economic reburning fuel owing to its lower energy cost. Research on coal has revealed that soot (Seeker et al. 1981) has provided heterogenous catalytic surface NO conversion. The U.S. Department of Energy and various industries, in

an effort to find a cleaner usage of coal, have established the Clean Coal Technology Demonstration Program (update 1991, Feb 92). Ever since, several solicitations have been issued and several solicited projects have been conducted in pursuit of innovative, energy efficient, economically competitive technologies responsive to the clean air act amendments of 1990.

1.2.2.2 Control of nitrogen oxides

Twenty million tons of nitrogen oxides are produced every year by various combustion processes. More than fifty percent of it is from the stationary combustion systems. Freihaut and Seery (1985) reported that during coal and lignite pyrolysis, HCN, not NH_3 was the primary pyrolysis product and a very small portion of coal nitrogen was converted to ammonia. Bose et al. (1988) demonstrated further that, under very short reaction time (< 1 sec) and 1 atm fuel rich oxidative environment (SR=0.6-0.8), NH_3 is derived from HCN and HCN from tar nitrogen. Their conclusion is drawn for coals of various rank, including lignite. These two pieces of work indicate that HCN is the primary pyrolysis product, which is subsequently converted into amine species, NO and N_2.

Heterogenous NO reduction on char or ash surface has also been demonstrated (De Soete, 1980). Its effectiveness is usually lower than the hydrocarbon gases, and therefore, is usually discarded when the stoichiometry is higher than 0.7. However, Burch et al. (1991a) found that the char derived from a North Dakota lignite had very high NO conversion (to HCN) efficiency, and the ash derived from the same lignite had very high HCN conversion (to NH_3) efficiency. While NH_3 is the dominant fixed nitrogen species during fuel rich combustion of lignite (Chen et al. 1982; Burch et al. 1991a), these results indicate that a char

conversion to HCN and HCN conversion to NH_3 may both be catalyzed by minerals (or other hydrocarbons) in the lignite. The North Dakota lignite ash used by Burch et al. has a very high (23%) content of calcium oxide.

Tsujimura et al (1983), in their studies on catalytic reduction of nitric oxide by carbon monoxide over calcined limestone, have found that calcined limestone has high catalytic activity for NO reduction by carbon monoxide and the obtained rate exceeds the rate of catalytic as well as non-catalytic reduction by char. Huffman et al. (1990), in their work on the behavior of basic elements during coal combustion have reported that calcium is molecularly dispersed in coal macerals and is bonded to the oxygen anions. This calcium present in lignite agglomerates and eventually forms CaO.

One of the objectives of this work was to study the effectiveness of CaC_2 and CaS in reducing NO under methane reburning conditions.

1.2.2.3 Heterogenous nitric oxide reduction mechanism

The literature contains a number of mechanisms on the char gasification by NO. These include Chan et al. (1983), Teng et al. (1992), and Levy et al. (1981).

Furasawa et al. (1980) in his work on NO reduction over char (produced by carbonization of the non-coking Taiheiyo coal) has reported that there is a change in the mechanism at 680C. They suggested the important NO reduction at high temperatures (> 680C) as

$$C + NO \text{-----} \frac{1}{2}N_2 + CO \qquad \textbf{(R5)}$$

From global kinetic data Chan et al. (1983) proposed the following reaction model

$$NO + C \text{-----} C(O) + \frac{1}{2}N_2 \qquad \textbf{(R6)}$$

$$CO + C(O) \text{-----} CO_2 + C \qquad \textbf{(R7)}$$

$$C(O) \text{-----} CO \qquad \textbf{(R8)}$$

where C represents a surface carbon, and the atoms inside the bracket represents adsorbed atoms. There is a general agreement that the first step (chemisorption of CO) is temperature independent. It probably involves addition of NO in an "N-down" configuration, followed by release of N_2 and formation of carbon oxide surface complexes. Reactions (R7) and (R8) represents the desorption steps of the surface oxides.

Teng et al. (1992) have suggested the following reaction mechanisms.

$$2C + NO \text{-----} C(O) + C(N) \qquad \textbf{(R9)}$$

$$C + C(O) + NO \text{-----} C(O_2) + C(N) \qquad \textbf{(R10)}$$

$$2C + 2NO \text{ -----} 2C(NO) \qquad \textbf{(R11)}$$

$$C(+ C(O) + NO \text{-----} CO_2 + C(N) + xC(\qquad \textbf{(R12)}$$

$$C(+ NO \text{-----} CO + C(N) + yC(\qquad \textbf{(R13)}$$

$$C(O) \text{-----} CO + aC(\qquad \textbf{(R14)}$$

$$C(O_2) \text{-----} CO_2 + bC(\qquad \textbf{(R15)}$$

$$2C(N) \text{-----} N_2 + dC(\qquad \textbf{(R16)}$$

Their interpretations on the above mechanisms are as follows: Reaction (R11) is only

important at low temperature (< 473 K). Reactions (R9) and (R10) are dissociative chemisorption on non-rapid turnover sites. The reactions involving C* are the rapid turnover sites reactions, that yield CO and CO_2. Reactions (R14), (R15), (R16) reflect formation of surface sites.

In summary Teng et al. (1992) have reported that carbon gasification by NO involves the desorption of surface complexes by a process such as (R8), i.e.,

$$[Surface\ \ Complexes] \qquad CO,\ CO_2,\ N_2 \qquad \textbf{(R17)}$$

but the product release process also involves the direct participation of NO in an apparently single step adsorption process.

$$C + NO \qquad CO,\ CO_2,\ N_2 \qquad \textbf{(R18)}$$

These two separate processes (R17) and (R18) are hypothesized to be linked through the existence of free sites, (created because of the faster desorption of products than product formation) that can rapidly turnover. They have also observed that unstable surface complexes form at low temperatures due to the NO attack on rapid turnover sites, and majority of them is found to be CO_2. It is reported that above 680C NO attacks char on active unoccupied sites that result in immediate desorption of gaseous products like N_2, CO, and CO_2. This process is reported to be controlled by dissociative chemisorption of NO on carbon surface. They suggested that the change in mechanism (activation energy) observed at 923K could be partially due to transition from slow desorption of surface complex, to release of the products from high turnover sites. They have also indicated that the number

of sites was affected by gasification temperature, but surface is not altered because of gasification temperature.

Levy et al. (1981) in their work on NO/char reactions at pulverized coal flame conditions have suggested that the reduction of NO by carbon is probably through dissociation of NO on the surface with a rapid surface diffusion of the dissociated atoms to form N_2. The oxygen produced by the dissociation is strongly chemisorbed and will inhibit further reaction, i.e.,

$$NO + 2C \text{----} C(N) + C(O) \qquad \textbf{(R19)}$$

$$C(N) + C(N) \text{----} N_2 + 2C \qquad \textbf{(R20)}$$

where C represents a surface carbon, C(N) and C(O) represent adsorbed nitrogen and oxygen atoms. The chemisorbed oxygen can either desorb to produce CO or react with CO to form CO_2, i.e.,

$$C(O) \text{----} CO \qquad \textbf{(R21)}$$

$$C(O) + CO \text{----} CO_2 + C \qquad \textbf{(R22)}$$

1.2.2.4 Dominant NO_X reduction mechanisms

Previous findings by Furasawa et al. (1985) on fate of fuel bond nitrogen, have suggested that the destruction of NO could be achieved through 1) gas-solid reactions (char consuming reaction), 2) gas-solid catalytic reactions (char catalytic reaction), and 3) gas phase homogenous reactions (CO+NO). Cowley and Roberts (1981) have reported that the gas phase reactions in nitric oxide reduction (third type) play a minor role and that the

absence of a major gas phase reaction of NO and coal nitrogen into N_2 requires the participation of a surface which catalyzes reactions (second type). Furasawa et al. (1982) reported that under fluidized bed combustion conditions, the use of carbon monoxide reduced the consumption of carbon in char approximately to zero and the char provided catalytic surfaces for nitric oxide reduction by carbon monoxide as

$$NO + CO \text{----} CO_2 + \frac{1}{2}N_2 \qquad \textbf{(R24)}$$

However, the effect of carbon monoxide on the "NO" reduction rate was reduced over the higher temperature range employed for fluidized combustion of coal. Levy et al. (1981) studied the NO/char reactions for pulverized coal flame conditions and reported slight enhancement (1.28 times higher) of the NO/char reaction rate with CO. Also, it is suggested that the increase in the rate may be due to an increase in active carbon sites by the removal of surface oxides as mentioned in (R22). As mentioned earlier, Furasawa et al. (1980) reported 98% conversion of carbon in char to CO during NO gasification at a temperature of approximately 910C. It was also mentioned that at higher temperatures, CO formation will be even higher. Levy et al. (1981) and Teng et al. (1992) have also reported that the primary product of the NO / char reaction at pulverised coal combustion conditions is CO. Therefore it could be possible that under pulverized bed combustion conditions, the major NO_x reducing mechanism is NO and char heterogenous reaction, and minor NO_x reducing mechanism is char catalyzed NO reduction.

A part of this work was to study the heterogenous NO reduction by char gasification.

1.3 Impacts of This Research on the Controls of NO_X

Although the fuel nitrogen is not oxidized with a high efficiency compared to fuel sulfur, acceptable concentrations of NO_x are much lower compared to those of SO_x. NO contributes to acid rain, photochemical smog, and is hazardous to health. Hence it has been imposed by federal regulations that the level of the national primary ambient air quality standards (NAAQS) for nitrogen dioxide (which is formed by reaction of NO with ozone in the atmosphere causing ozone depletion) is 0.053 parts per million or 100 micrograms per cubic meter (Code of federal regulations, 1991). The Clean Air Act Amendment (CAAA) is imposed to attain National Ambient Air Quality Standards (NAAQS). The main objective of CAAA was to reduce volatile organic compounds by 15% by 1996. Following 1996, a 3% per year reduction of NO_x was required of serious, severe, and extreme areas; the area classification based on degree of containment of pollution. But the most stringent regulations are laid out by state air pollution control agencies called NO_x Reasonably Achievable Control Technology (RACT). According to this, states with ozone non-attainment areas classified as serious, severe or extreme should not emit more than 50, 25 and 10 tons/yr per individual unit (The Clean Air Advisor, Sep 92) respectively. Hence, in order to control the air quality standards, various NO_x emission control strategies have been evolved.

The research conducted under this grant instrument was an attempt to reduce NO_x emissions, below allowable standards.

1) The hybrid technology of reburning and non-selective catalytic reduction is expected to reduce NO_x significantly. Also this hybrid technology is expected to be cost

effective.

2) The reduction of NO by CaC_2/CaS active catalyst surface under methane reburning conditions is expected to find cleaner ways of NO_x reduction and promote the utility of CaC_2/CaS. Also usage of CaC_2/CaS as active catalyst surface can play a vital role in the reduction of soot emissions.

3) The NO reduction by lignite char will find wider utility value for coal. Also the deduction of the char reduction mechanism will promote the understanding of NO_x reduction mechanism and therefore its reduction.

The following chapters will describe the computational modeling and experimental studies performed under this grant instrument. Chapter II presents the work planned and Chapter III focusses on the computational modeling. Chapter IV describes the experimental facility and how it was designed. Chapter V presents the results of all the experimental studies conducted at the Rust College Testing Facility. The conclusions and recommendations are given in Chapter VI.

Chapter II

STATEMENT OF WORK

This chapter presents the statement of work proposed and performed under the grant instrument. The tasks proposed are given in Section 2.1. Section 2.2 outlines the various phases of the work performed. These include both numerical modeling and experimental studies.

2.1 Proposed Work

The following is the statement of work submitted (quoted verbatim) when the grant instrument began in February 1995.

Task 1. Computer Simulation Studies and Experimental Design

Computer simulation studies will be used to aid in the development of a series of experiments that will extend our knowledge of the reburning process and as a tool to understand the results obtained from experimental findings.

Experiments aimed at furthering the understanding of the mechanisms involved in reburning reactions will be postulated. Computer simulation studies using the CHEMKIN kinetic analysis package and other modeling tools shall be conducted to determine the degree to which these experiments would further our understanding of NO_x reduction in coal combustion systems.

Information obtained from the modeling studies and further examination of literature shall, be used to carefully and thoughtfully plan a series of experiments that will extend our knowledge of the reburning process.

As experimental results become available, additional computer simulation studies will be conducted to gain a deeper understanding of the findings and determine how the results could be applied to full-scale combustors.

Task 2. Experimental Studies

A series of experiments designed in Task 1 shall be performed. These experiments could involve, but are not limited to:

* the reduction of nitric oxide using a combination of methane and acetylene

* hybrid technology- reburning with methane and selective non-catalytic reduction with ammonia

* surface catalyzed reburning studies- employing CaC_2, CaS, and other materials as active catalyst surfaces, and

* char gasification studies.

Task 3. Reporting and Management

All required reports and deliverables shall be prepared according to the schedule and instructions provided.

2.2 Computer Simulation Studies

The research team performed extensive computer simulation studies on homogeneous, gas-phase combustion that provided a valuable information on planning a series of experiments during the course of the grant instrument. The simulation studies and the experimental work were dovetailed and they overlapped several times to aid the research team in the experimental design as well as the actual experimentation. The results of computer

simulation studies is documented in Chapter III.

2.3 Experimental Design and Facility

A detailed design of the experimental facility developed under this grant instrument is documented in Chapter IV, which outlines the choice of reactor, the particular reactor geometry to meet the conditions, various pieces of equipment that are integral part of the facility and the design of coal feeder that was a crucial part for the heterogeneous reactions.

2.4 Experimental Studies

The experimental studies can be broadly classified as homogeneous gaseous reburning experiments (NO_x reduction using a combination of methane and acetylene and reburning with methane and selective non-catalytic reduction with ammonia) and heterogeneous experiments (surface catalyzed reburning and char gasification).

2.4.1 Homogeneous reburning experiments

Presented in Fig. 2.1 is the general experimental setup used for the homogeneous reburning experiments with methane, a combination of methane and acetylene and a combination of methane and ammonia. The experimental facility is described in detail in Chapter IV. Listed in Table 2.1 is the test matrix for this phase of homogeneous combustion which yielded the extent of NO reduction with the above reburning fuels. The focus was to find the operating point, that is, what reburning stoichiometric ratio (SR2) is optimum out of SR2 range 0.8-1.0. The results are summarized in Chapter V, Section 5.1.

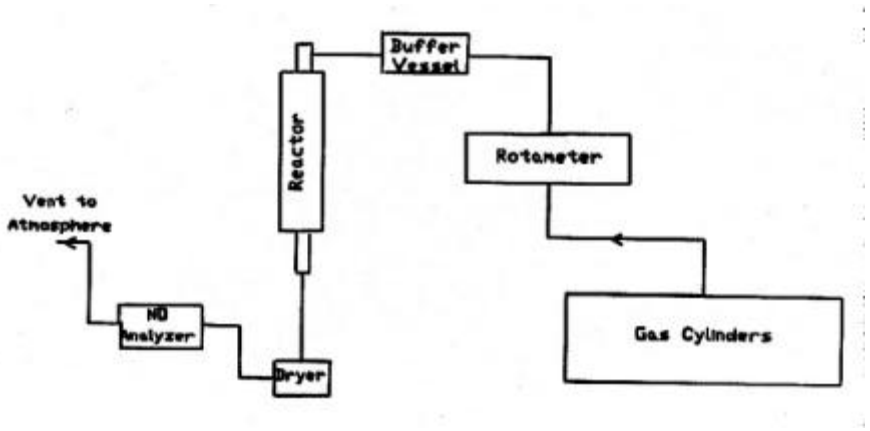

Figure 2.1 Experimental setup for homogeneous combustion experiments

Table 2.1 Test matrix for homogeneous, gas-phase combustion experiments

Experiment	Test conditions	Objective of the test	No. of runs
1.Reburning with CH_4 (Validity tests for the experimental facility)	a. Temp=1373 K Pressure=1 atm. Reburning Stoichio-metric ratios (SR2): 0.8,0.85,0.9, 0.95,1.0	To test if our experimental setup can achieve what is projected in computer runs & previous researchers' experiments.	SR2= 0.8, 0.85,0.9, 0.95,1.0. 5 runs
	b. Same as 1a but Temp=1273 K	To test if lowering temperature has any impact.	5 runs
	c. Same as 1b But Temp=1423 K	To test if increasing temperature has any impact.	5 runs

2.Reburning with CH_4/C_2H_2	a. Temp=1373 K or best operating temp point from 1b & 1c. Pressure= 1 atm. CH_4=90% and C_2H_2=10% SR2=0.8,0.85,0.9, 0.95,1.0	To reduce NO to levels below what CH_4 can individually achieve.	5 runs
	b. Same as 2a but CH_4=80%,C_2H_2=20%	To see if we can get better reduction than 2a.	5 runs
	c. Interpret from 2a & 2b as what will be best CH_4=?,C_2H_2 =?. (95/5, 90/10, 85/15)	To keep the utility cost of C_2H_2 down at the same time achieving the necessary NO reduction.	15 runs
3.Reburning with CH_4 & non-selective catalytic reduction with NH_3	a.Temp=1373 K or best operating point from 1b & 1c. Pressure= 1 atm. SR2=0.8,0.85,0.9, 0.95,1.0. CH_4=98% NH_3=2%	To reduce NO to levels below what CH_4 can individually achieve. To find if it will be better than CH_4 &C_2H_2 i.e 2a &2b.	5 runs
	b.same as 3a but CH_4=96%,NH_3=4%	To find if we can get better reduction.	5 runs

2.4.2 Heterogeneous combustion experiments

Presented in Fig. 2.2 is the general experimental setup used for the heterogeneous combustion reburning experiments. The experimental facility is described in detail in Chapter IV. Heterogeneous combustion tests were planned to be conducted at SR2=0.95 to see how various solid particles fed through the coal feeder impacted NO reduction by methane. These

tests included the following.

A. Reburning studies with methane and coal.

The coal samples tested were 1) a high volatile A bituminous Pittsburgh coal (DECS-23 from PennState Coal Sample Databank), 2) C bituminous Illinois coal (DECS-24), 3) Montana lignite coal (DECS-25).

B. Reburning studies with methane and activated carbon (char gasification).

C. Surface catalyzed reburning studies.

The experiments were performed with 1) calcium sulfide and 2) calcium carbide to see their catalytic effect on NO reduction.

The results of the above experiments are summarized in Chapter V, Section 5.2.

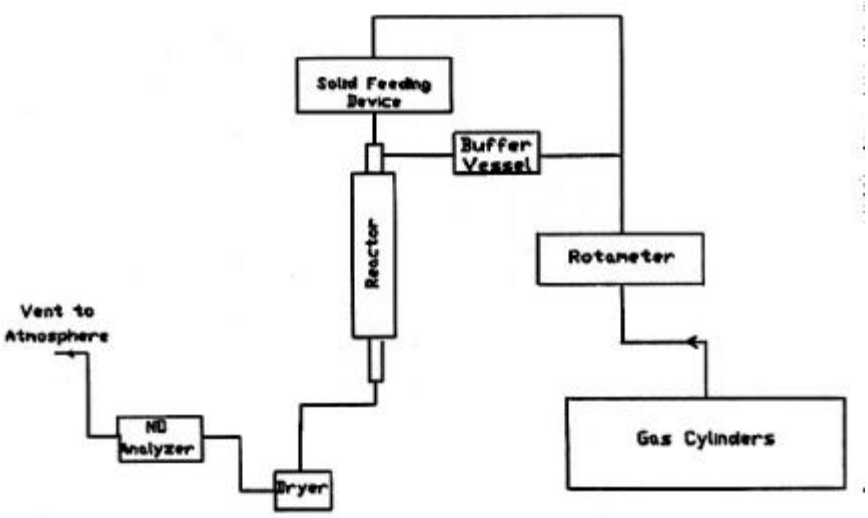

Figure 2.2 Experimental setup for heterogeneous combustion experiments

The subsequent chapters detail the work performed under this grant instrument.

Chapter III

COMPUTATIONAL MODELING

Right from the inception of the grant, computer simulation studies were undertaken to aid in planning and conducting a series of experiments that would extend our knowledge of reburning process. These studies would be the pointers for setting up the appropriate experimental facility and planning the test runs wisely. As a starting point for this phase, the updated version of CHEMKIN II (1994) package was acquired from Sandia National Laboratories and put to use for the preliminary runs involving reburning of nitric oxide with methane.

3.1 Reaction Mechanism

A detailed reaction mechanism involving hydrocarbon and nitrogen containing species was prepared to study reburning. This is very similar to that of Kilpinen et al (1992). While constant efforts were made to update this mechanism based on the most recent literature, the preliminary runs on reburning with methane showed promising results. Listed in Table 3.1 is the reaction mechanism used for the computations that follow.

The reaction mechanism was updated constantly. Existing rate constants data were checked against several recent publications which included (a) a paper by Byrne and Dean (1993) who used a large hydrocarbon mechanism that consisted of 497 reactions and 135 species, (b) summary table of evaluated kinetic data for combustion modeling by Baulch et al (1994), © specific reaction rate constants for CH_4 - O_2 system used by Lee and Chung (1994), (d) ammonia oxidation reaction mechanism employed by Vandooren et al (1994), (e)

detailed kinetic modeling of chemistry and temperature effects on ammonia oxidation by Lindstedt et al (1994) and (f) several mechanism and modeling studies conducted by Glargborg et al (1994a,b,c).

Table 3.1 Reaction mechanism used for reburning with methane and acetylene

REACTIONS CONSIDERED	(k = A T**b exp(-E/RT)) A	b	E
1. C2H6+M=2CH3+M	5.80E+13	0.0	75000.0
2. CH4+M=CH3+H+M	4.17E+17	0.0	92300.0
H2O Enhanced by 5			
3. CH4+O2=CH3+HO2	4.00E+13	0.0	56910.0
4. CH4+H=CH3+H2	2.02E+04	3.0	8750.0
5. CH4+OH=CH3+H2O	1.90E+05	2.4	2110.0
6. CH4+O=CH3+OH	1.02E+09	1.5	8604.0
7. CH4+HO2=CH3+H2O2	1.80E+11	0.0	18700.0
8. CH4+CH2=CH3+CH3	4.30E+13	0.0	10030.0
9. CH3+CH2O=CH4+HCO	5.50E+03	2.8	5860.0
10. CH3+HCO=CH4+CO	1.20E+14	0.0	0.0
11. CH3+M=CH2+H+M	1.90E+16	0.0	91600.0
12. CH3+HO2=CH3O+OH	2.00E+13	0.0	0.0
13. CH3+O2=CH3O+O	2.05E+19	-1.6	29229.0
14. CH3+O=CH2O+H	8.40E+13	0.0	0.0
15. CH3+OH=CH2+H2O	7.50E+06	2.0	5000.0
16. CH3+H=CH2+H2	9.00E+13	0.0	15100.0
17. CH3O+M=CH2O+H+M	1.00E+14	0.0	25000.0
18. CH2OH+M=CH2O+H+M	1.00E+14	0.0	25000.0
19. CH3O+H=CH2O+H2	2.00E+13	0.0	0.0
20. CH2OH+H=CH2O+H2	3.00E+13	0.0	0.0
21. CH3O+OH=CH2O+H2O	1.00E+13	0.0	0.0
22. CH2OH+OH=CH2O+H2O	1.00E+13	0.0	0.0
23. CH3O+O=CH2O+OH	1.00E+13	0.0	0.0
24. CH2OH+O=CH2O+OH	1.00E+13	0.0	0.0
25. CH3O+O2=CH2O+HO2	6.30E+10	0.0	2600.0
26. CH2OH+O2=CH2O+HO2	1.48E+13	0.0	1500.0
27. CH2+HCO=CH3+CO	2.00E+13	0.0	0.0
28. CH2+H=CH+H2	1.00E+17	-1.2	0.0
29. CH2+OH=CH+H2O	1.13E+07	2.0	3000.0

30. CH2+OH=CH2O+H	3.00E+13	0.0	0.0
31. CH+O2=HCO+O	3.30E+13	0.0	0.0
32. CH+O=CO+H	1.00E+13	0.3	0.0
33. CH+OH=HCO+H	5.00E+13	0.0	0.0
34. CH+CO2=HCO+CO	3.40E+12	0.0	690.0
35. CH+H=C+H2	1.50E+14	0.0	0.0
36. CH+H2O=CH2O+H	5.70E+12	0.0	-755.0
37. CH+CH2O=CH2CO+H	9.46E+13	0.0	-515.0
38. CH+C2H2=C3H2+H	8.40E+13	0.0	0.0
39. CH+CH2=C2H2+H	4.00E+13	0.0	0.0
40. CH+CH3=C2H3+H	3.00E+13	0.0	0.0
41. CH+CH4=C2H4+H	6.00E+13	0.0	0.0
42. C+O2=CO+O	2.00E+13	0.0	0.0
43. C+OH=CO+H	5.00E+13	0.0	0.0
44. C+CH3=C2H2+H	5.00E+13	0.0	0.0
45. C+CH2=C2H+H	5.00E+13	0.0	0.0
46. CH2+CO2=CH2O+CO	1.10E+11	0.0	1000.0
47. CH2+O=CO+2H	1.70E+13	0.2	0.0
48. CH2+O=CO+H2	9.00E+12	0.2	0.0
49. CH2+O2=CO2+2H	1.60E+12	0.0	1000.0
50. CH2+O2=CH2O+O	5.00E+13	0.0	9000.0
51. CH2+O2=CO2+H2	6.90E+11	0.0	500.0
52. CH2+O2=CO+H2O	1.90E+10	0.0	-1000.0
53. CH2+O2=CO+OH+H	8.60E+10	0.0	-500.0
54. CH2+O2=HCO+OH	4.30E+10	0.0	-500.0
55. CH2O+M=CO+H2+M	8.30E+15	0.0	69550.0
56. CH2O+O=CO2+2H	3.50E+05	2.4	1360.0
57. CH2O+OH=HCO+H2O	3.43E+09	1.2	-447.0
58. CH2O+H=HCO+H2	2.19E+08	1.8	3000.0
59. CH2O+M=HCO+H+M	1.00E+16	0.0	80270.0
60. CH2O+O=HCO+OH	1.70E+16	2.3	3080.0
61. HCO+OH=H2O+CO	1.00E+14	0.0	0.0
62. HCO+H=CO+H2	1.19E+13	0.3	0.0
63. HCO+O=CO+OH	3.00E+13	0.0	0.0
64. HCO+O=CO2+H	3.00E+13	0.0	0.0
65. HCO+O2=HO2+CO	3.30E+13	-0.4	0.0
66. CO+O+M=CO2+M	6.17E+14	0.0	3000.0
67. CO+OH=CO2+H	1.51E+07	1.3	-758.0
68. CO+O2=CO2+O	2.50E+12	0.0	47700.0
69. HO2+CO=CO2+OH	5.80E+13	0.0	22934.0
70. C2H6+CH3=C2H5+CH4	5.50E-01	4.0	8300.0
71. C2H6+H=C2H5+H2	5.40E+02	3.5	5210.0
72. C2H6+O=C2H5+OH	1.20E+12	0.6	7310.0

73. C2H6+OH=C2H5+H2O	8.70E+09	1.0	1810.0
74. C2H4+OH=CH2O+CH3	5.60E+12	0.0	1500.0
75. C2H4+CH3=C2H3+CH4	6.60E+00	3.7	9500.0
76. C2H4+H=C2H3+H2	1.30E+06	2.5	12240.0
77. C2H4+OH=C2H3+H2O	9.00E+13	0.0	6860.0
78. CH2+CH3=C2H4+H	4.20E+13	0.0	0.0
79. C2H5+M=C2H4+H+M	1.00E+17	0.0	31000.0
80. C2H5+H=2CH3	2.30E+12	0.5	0.0
81. C2H5+O2=C2H4+HO2	8.43E+11	0.0	3875.0
82. C2H2+O=CH2+CO	1.70E+08	1.6	2210.0
83. C2H2+O=HCCO+H	2.50E+08	1.6	2210.0
84. H2+C2H=C2H2+H	4.09E+05	2.4	864.0
85. C2H3+M=C2H2+H+M	8.00E+14	0.0	31550.0
86. C2H3+H=C2H2+H2	4.00E+13	0.0	0.0
87. C2H3+O=CH2CO+H	3.30E+13	0.0	0.0
88. C2H3+O2=C2H2+HO2	4.00E+12	0.0	-250.0
89. C2H3+OH=C2H2+H2O	5.00E+12	0.0	0.0
90. OH+C2H2=C2H+H2O	3.37E+07	2.0	14000.0
91. OH+C2H2=CH2CO+H	2.18E-04	4.5	-1000.0
92. CH2CO+H=CH3+CO	1.13E+13	0.0	3428.0
93. CH2CO+H=HCCO+H2	5.00E+13	0.0	8000.0
94. CH2CO+O=HCCO+OH	1.00E+13	0.0	8000.0
95. CH2CO+O=CH2O+CO	1.50E+12	0.0	1350.0
96. CH2CO+OH=HCCO+H2O	7.50E+12	0.0	3000.0
97. CH2CO+M=CH2+CO+M	1.50E+15	0.0	57600.0
98. C2H+O2=CO+HCO	5.00E+13	0.0	1500.0
99. C2H+C2H2=C4H2+H	4.00E+13	0.0	0.0
100. O+HCCO=H+2CO	1.00E+14	0.0	0.0
101. HCCO+O2=2CO+OH	1.60E+12	0.0	854.0
102. CH+HCCO=C2H2+CO	5.00E+13	0.0	0.0
103. 2HCCO=C2H2+2CO	1.00E+13	0.0	0.0
104. C2H+O=CH+CO	5.00E+13	0.0	0.0
105. C2H+OH=HCCO+H	2.00E+13	0.0	0.0
106. 2CH2=C2H2+2H	1.00E+12	0.6	0.0
107. CH2+HCCO=C2H3+CO	3.00E+13	0.0	0.0
108. C4H2+OH=C3H2+HCO	3.00E+13	0.0	0.0
109. C3H2+O2=HCO+HCCO	1.00E+13	0.0	0.0
110. C4H2+O=C3H2+CO	2.70E+13	0.0	1700.0
111. C2H2+M=C2H+H+M	4.20E+16	0.0	107000.0
112. C2H4+M=C2H2+H2+M	1.50E+15	0.0	55440.0
113. C2H4+M=C2H3+H+M	1.40E+16	0.0	81280.0
114. H2+O2=2OH	1.70E+13	0.0	47780.0
115. OH+H2=H2O+H	6.40E+06	2.0	2961.0

116. O+OH=O2+H		4.50E+14	-0.5	600.0
117. O+H2=OH+H		5.06E+04	2.7	6290.0
118. H+O2+M=HO2+M		7.00E+17	-0.8	0.0
H2O	Enhanced by 18.6			
CO2	Enhanced by 4.2			
H2	Enhanced by 2.86			
CO	Enhanced by 2.11			
N2	Enhanced by 1.26			
119. H+HO2=2OH		2.50E+14	0.0	1900.0
120. O+HO2=OH+O2		4.80E+13	0.0	1000.0
121. OH+HO2=H2O+O2		5.00E+13	0.0	1000.0
122. 2OH=O+H2O		2.10E+08	1.4	-400.0
123. 2H+M=H2+M		1.00E+18	-1.0	0.0
H2	Enhanced by 0			
H2O	Enhanced by 0			
CO2	Enhanced by 0			
124. 2H+H2=2H2		9.20E+16	-0.6	0.0
125. 2H+H2O=H2+H2O		6.00E+19	-1.3	0.0
126. 2H+CO2=H2+CO2		5.49E+20	-2.0	0.0
127. H+OH+M=H2O+M		7.50E+23	-2.6	0.0
H2O	Enhanced by 5			
128. 2O+M=O2+M		1.89E+13	0.0	-1788.0
129. H+HO2=H2+O2		2.50E+13	0.0	700.0
130. 2HO2=H2O2+O2		2.00E+12	0.0	0.0
131. H2O2+M=2OH+M		1.20E+17	0.0	45500.0
132. H2O2+H=HO2+H2		1.70E+12	0.0	3750.0
133. H2O2+O=HO2+OH		9.60E+06	2.0	3974.0
134. H2O2+OH=H2O+HO2		1.00E+13	0.0	1800.0
135. CH+N2=HCN+N		3.00E+11	0.0	13600.0
136. CN+N=C+N2		1.90E+15	-0.6	0.0
137. CH2+N2=HCN+NH		1.00E+13	0.0	74000.0
138. H2CN+M=HCN+H+M		3.00E+14	0.0	22000.0
139. C+NO=CN+O		3.70E+13	0.0	0.0
140. CH+NO=HCN+O		1.10E+14	0.0	0.0
141. CH2+NO=HCNO+H		1.39E+12	0.0	-1100.0
142. CH3+NO=HCN+H2O		5.30E+11	0.0	15000.0
143. CH3+NO=H2CN+OH		5.30E+11	0.0	15000.0
144. HCCO+NO=HCNO+CO		2.00E+13	0.0	0.0
145. HCNO+H=HCN+OH		1.00E+14	0.0	12000.0
146. HNCO+O=NCO+OH		3.20E+12	0.0	10300.0
147. HNCO+OH=NCO+H2O		2.60E+12	0.0	5540.0
148. CH2+N=HCN+H		5.00E+13	0.0	0.0
149. CH+N=CN+H		1.30E+13	0.0	0.0

150. CO2+N=NO+CO	1.90E+11	0.0	3400.0
151. HCCO+N=HCN+CO	5.00E+13	0.0	0.0
152. CH3+N=H2CN+H	3.00E+13	0.0	0.0
153. C2H3+N=HCN+CH2	2.00E+13	0.0	0.0
154. HCN+OH=CN+H2O	1.45E+13	0.0	10929.0
155. OH+HCN=HOCN+H	5.85E+04	2.4	12500.0
156. OH+HCN=HNCO+H	1.98E-03	4.0	1000.0
157. OH+HCN=NH2+CO	7.83E-03	4.0	4000.0
158. HOCN+H=HNCO+H	1.00E+13	0.0	0.0
159. HCN+O=NCO+H	1.38E+04	2.6	4980.0
160. HCN+O=NH+CO	3.45E+03	2.6	4980.0
161. HCN+O=CN+OH	2.70E+09	1.6	29200.0
162. CN+H2=HCN+H	2.95E+05	2.5	2237.0
163. CN+O=CO+N	1.80E+13	0.0	0.0
164. CN+O2=NCO+O	5.60E+12	0.0	0.0
165. CN+OH=NCO+H	6.00E+13	0.0	0.0
166. HO2+NO=NO2+OH	2.11E+12	0.0	-479.0
167. NO2+H=NO+OH	3.50E+14	0.0	1500.0
168. NO2+O=NO+O2	1.00E+13	0.0	600.0
169. NO2+M=NO+O+M	1.10E+16	0.0	66000.0
170. NCO+H=NH+CO	5.00E+13	0.0	0.0
171. NCO+O=NO+CO	3.20E+13	0.0	0.0
172. NCO+N=N2+CO	2.00E+13	0.0	0.0
173. NCO+OH=NO+CO+H	1.00E+13	0.0	0.0
174. NCO+M=N+CO+M	3.10E+16	-0.5	47700.0
175. NCO+NO=N2O+CO	1.00E+13	0.0	-390.0
176. NCO+H2=HNCO+H	8.58E+12	0.0	9000.0
177. HNCO+H=NH2+CO	1.10E+14	0.0	12720.0
178. NH+O2=HNO+O	1.00E+13	0.0	12000.0
179. NH+O2=NO+OH	7.60E+10	0.0	1530.0
180. NH+O=NO+H	2.00E+13	0.0	0.0
181. NH+NO=N2O+H	2.40E+15	-0.8	0.0
182. N2O+OH=N2+HO2	2.00E+12	0.0	10000.0
183. N2O+H=N2+OH	1.90E+06	2.4	13500.0
184. N2O+M=N2+O+M	9.30E+14	0.0	59300.0
185. N2O+O=N2+O2	1.00E+14	0.0	28200.0
186. N2O+O=2NO	1.00E+14	0.0	28200.0
187. NH+OH=HNO+H	2.00E+13	0.0	0.0
188. NH+OH=N+H2O	5.00E+11	0.5	2000.0
189. NH+H=N+H2	1.00E+14	0.0	0.0
190. NH2+O=HNO+H	7.90E+14	-0.5	0.0
191. NH2+O=NH+OH	7.00E+12	0.0	0.0
192. NH2+OH=NH+H2O	4.00E+06	2.0	1000.0

193. NH2+H=NH+H2	6.92E+13	0.0	3650.0
194. NH2+NO=NNH+OH	6.40E+15	-1.3	0.0
195. NH3+OH=NH2+H2O	2.04E+06	2.0	566.0
196. NH3+H=NH2+H2	6.36E+05	2.4	10171.0
197. NH3+M=NH2+H+M	1.40E+16	0.0	90600.0
198. NNH=N2+H	1.00E+04	0.0	0.0
199. NNH+NO=N2+HNO	5.00E+13	0.0	0.0
200. NNH+H=N2+H2	1.00E+14	0.0	0.0
201. NNH+OH=N2+H2O	5.00E+13	0.0	0.0
202. NNH+O=N2O+H	1.00E+14	0.0	0.0
203. HNO+M=H+NO+M	1.50E+16	0.0	48680.0
H2O Enhanced by 10			
O2 Enhanced by 2			
N2 Enhanced by 2			
H2 Enhanced by 2			
204. HNO+OH=NO+H2O	3.60E+13	0.0	0.0
205. HNO+H=H2+NO	5.00E+12	0.0	0.0
206. N+NO=N2+O	3.27E+12	0.3	0.0
207. N+O2=NO+O	6.40E+09	1.0	6280.0
208. N+OH=NO+H	3.80E+13	0.0	0.0
209. NO+NH2=N2O+H2	5.00E+13	0.0	24640.0
210. NO+N2H2=N2O+NH2	3.00E+12	0.0	0.0
211. NO2+NH2=N2O+H2O	1.90E+20	-3.0	0.0
212. HNO+NO=N2O+OH	2.00E+12	0.0	26000.0
213. HNO+HNO=N2O+H2O	4.00E+12	0.0	5000.0
214. N2O+CO=N2+CO2	5.00E+13	0.0	44000.0
215. HCCO+OH=HCO+CO+H	1.00E+13	0.0	0.0
216. HCO+M=CO+H+M	2.50E+14	0.0	16802.0
217. NH3+O=NH2+OH	2.10E+13	0.0	9000.0
218. NO+NH2=N2+H2O	6.20E+15	-1.3	0.0

NOTE: A units mole-cm-sec-K, E units cal/mole

3.2 Computational Method/Tool

The updated version of CHEMKIN II, acquired from Sandia National Laboratories, was loaded on the CRAY-Y MP Supercomputer located in the University of Mississippi. This employs VODE, an updated version of LSODE to solve the initial value problem for stiff

or nonstiff systems of first order ordinary differential equations.

Our research team employed an adiabatic system with constant pressure to define the reactor for NO reburning with methane. The input concentrations for various reburning stoichiometric ratios (0.7 to 1.05) were calculated and supplied to the program. The CHEMKIN package handles the chemical reaction mechanism (which is given in the previous section) and then allows VODE to calculate the temperature and species concentrations at various residence times.

We used SENKIN program also to solve this initial value problem which gave identical results. The program SENKIN uses the DASAC software to solve the nonlinear ODE that describe the temperature and species concentrations.

3.3 Results on NO Reburning with Methane

A typical input concentration for stoichiometric ratio (SR2)=0.7 is 15.9% CO_2, 1.83% O_2, 1000 ppm NO, 5.38% CH_4, and 76.79% inert gas. Similarly SR2=0.9 would represent the composition of flue gas as 16.45% CO_2, 1.87% O_2, 1000 ppm NO, 2.14% methane and 79.42% N_2/He. With varying SR2 conditions the program is run for three residence times (0.1 s, 0.2 s and 0.3 s) at the reactor temperature of 1373 K (1100 C). Also, the program is run for three temperatures, (1000 C, 1100 C and 1200 C) keeping the residence time as 0.2 s. The concentrations of NO_2 and N_2O were found to be negligible for all the cases. The three nitrogen containing species that are significant are NO, HCN and NH_3 and the concentrations of each versus SR2 are shown in the following figures.

Figures 3.1 through 3.3 show the exit concentrations of NO, HCN and NH_3 respectively for the reactor temperature of 1373 K at varying residence times, i.e., 0.1 s, 0.2 s and 0.3 s. It can be observed that the greatest reduction of NO into mainly HCN and to some extent NH_3 takes place at the reburning stoichiometric ratio of 0.9. This reduction is very significant as Figure 3.1 depicts, with NO concentration being 46 ppm at 0.2 s. This phenomenon is consistent with what other researchers have observed in the past. Both HCN and NH_3 show opposite trend with NO.

The NO reduction at 0.2 s residence time is considerably higher than the reduction at 0.1 s for stoichiometric ratios ranging from 0.7 to 0.9. However, there is no difference in NO reduction above SR2 value of 0.9. It can also be noticed that NO reduction is not much higher for the residence time of 0.3 s when compared with the reduction at 0.2 s. This difference is insignificant. Hence 0.2 s is chosen to be the optimum residence time for the reaction. This piece of finding was utilized in the reactor design later on as the grant instrument progressed. Also, the residence time of 0.2 s was found to be appropriate for experimental runs to account for non-idealities and to ensure that the equilibrium reaction for NO reduction proceeded to completion.

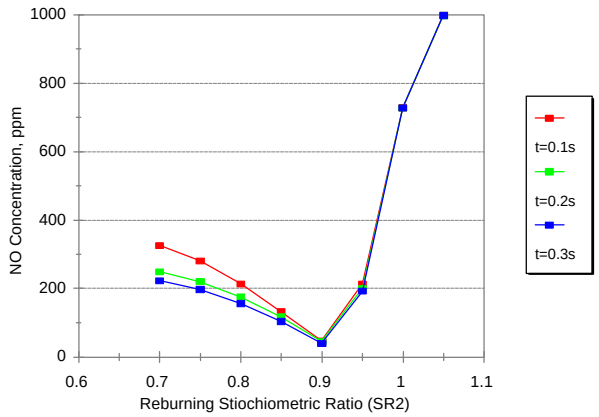

Figure 3.1 Effect of residence time on NO exit concentration in reburning by methane (Input NO Concentration: 1000 ppm; Reactor Temperature: 1373 K)

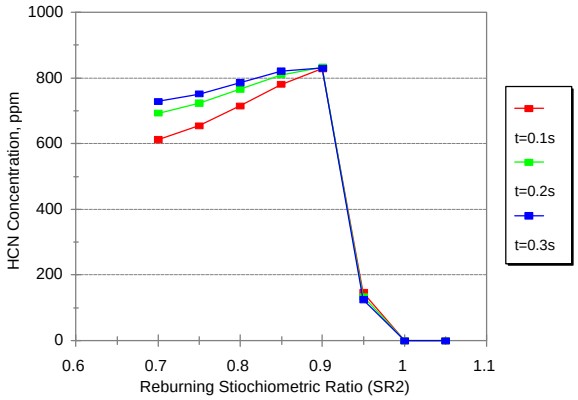

Figure 3.2 Effect of residence time on HCN exit concentration in reburning by methane (Input NO Concentration: 1000 ppm; Reactor Temperature: 1373 K)

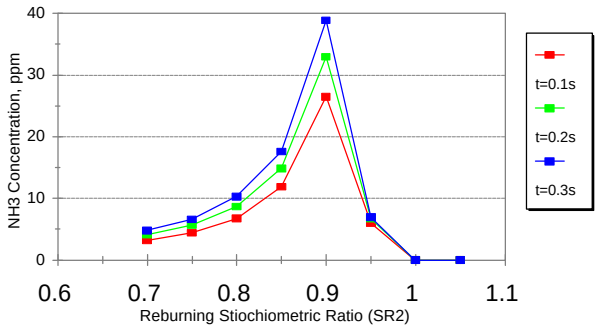

Figure 3.3 Effect of residence time on NH_3 exit concentration in reburning by methane (Input NO Concentration: 1000 ppm; Reactor Temperature: 1373 K)

Figures 3.4 through 3.6 depict the exit concentrations of NO, HCN, and NH_3 respectively for a residence time of 0.2 s for varying reactor temperature. The three temperatures are 1273 K, 1373 K and 1473 K. The trends are similar for all reactor temperatures. The greatest reduction of NO occurs at SR2=0.95 for lower temperatures (1273 K) and at SR2=0.9 for higher temperatures (1373 K and 1473 K). The concentration of HCN increases with increase in reactor temperature for the range 0.7 to (0.85-0.9) while it does the opposite for SR2 of 0.9-0.95. Probably this would mean that there is a shift in the mechanism at SR2 value in the neighborhood of 0.85-0.95. At SR2 < 0.9 the HCN formation is more from NO (70-80%). But above SR2 of 0.9, the NO→HCN mechanism is affected and hence the NO concentration goes up and HCN concentration goes down. Both HCN and NH_3 show similar trend with SR2, that is, as long as HCN is formed more, there is a corresponding increase in NH_3. This would mean a fragmental portion of HCN is always

converted to NH_3 by some reaction. Above SR2=0.9 the HCN formation decreases and so does the NH_3. Therefore we can postulate that NO reduction goes through a series reaction as follows: NO➔HCN➔NH_3.

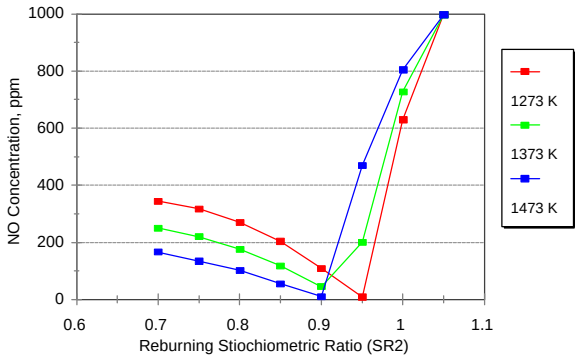

Figure 3.4 Effect of reactor temperature on NO exit concentration in reburning by methane (Input NO Concentration: 1000 ppm; Residence Time: 0.2 s)

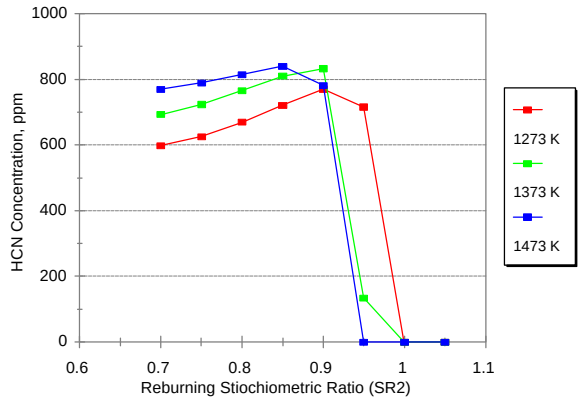

Figure 3.5 Effect of reactor temperature on HCN exit concentration in reburning by methane (Input NO Concentration: 1000 ppm; Residence Time: 0.2 s)

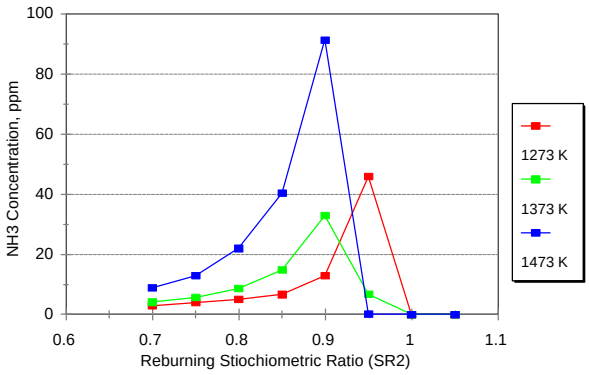

Figure 3.6 Effect of reactor temperature on NH_3 exit concentration in reburning by methane (Input NO Concentration: 1000 ppm; Residence Time: 0.2 s)

3.4 Results on NO Reburning with Methane and Acetylene

Presented herein are the computational results of NO reburning with a combination of methane and acetylene, employing the reaction mechanism listed in Table 3.1. Figures 3.7 through 3.9 portray these results.

The legends in Figures 3.7 through 3.9 describe the reburn fuel composition between methane and acetylene. A typical CH_4/C_2H_2: 90/10 combination at SR2=0.9 would represent the initial concentration of flue gas as 1.88% CH_4, 0.21% C_2H_2, 16.47% CO_2, 1.89% O_2, 1000 ppm NO and 79.45% N_2/He. With varying SR2 conditions, the program is run for a fixed reburn fuel composition for a residence time of 0.2 s at the reactor temperature of 1373 K. The final concentrations of various nitrogen containing species are obtained from these tests. Then another reburn fuel composition (say, 70/30) is chosen, the initial concentrations

of various species at different SR2 values (0.7 through 1.05) are calculated based on stoichiometry analysis and fed to the CHEMKIN to solve for the exit concentrations of nitrogen containing species at this reburn fuel composition. Likewise, the tests are repeated for various combinations of methane and acetylene. The three nitrogen containing species that are significant are NO, HCN and NH_3. The concentrations of NO_2 and N_2O were found to be negligible as in the case of methane reburning. Figures 3.7 through 3.9 are the result of 48 computer runs (6 reburn fuel compositions X 8 SR2 conditions) on the CHEMKIN. These figures display the effect of the composition of CH_4/C_2H_2 on exit concentrations of NO, HCN and NH_3 respectively in NO reburning.

The addition of acetylene to methane as reburn fuel seems to favor the reduction of NO appreciably, as seen in Fig. 3.7. The best achievable NO concentration for 100/0 combination of CH_4/C_2H_2 is 46 ppm from the initially fed 1000 ppm, as the equilibrium comes to completion . But with 10% acetylene, that is, 90/10 combination of CH_4/C_2H_2, we are able to obtain the much needed further reduction by shifting the equilibrium. For the 90% CH_4 and 10% C_2H_2 the concentration of NO is reduced from 1000 ppm to 7 ppm. This is very significant and contributes greatly toward meeting the regulations on NO_x reduction. From Fig. 3.8, it can be seen that HCN concentration is increased only slightly for 90% CH_4 and 10% C_2H_2 reaction (864 ppm) in comparison with the 100% CH_4 reaction (833 ppm). This HCN is highly unstable at high temperatures and its recovery is reported to be 30% at 1100 C for a residence time of 1 s (Song et al. 1982).

For all the reburn fuel combinations between CH_4 and C_2H_2 the variation of exit concentrations with SR2 values shows trends that are similar. At SR2 < 0.9 the HCN

formation is more from NO (70 - 90%). But above SR2 of 0.9, the NO➔HCN mechanism is greatly affected, that is, at SR2 > 0.9 the NO concentration increases and HCN concentration decreases. Both HCN and NH_3 show similar trend with SR2. It appears from Figures 3.8 and 3.9 that a fragmental portion of HCN is always converted to NH_3 by some reaction. The NO reduction could go through a series reaction NO➔HCN➔NH_3. Further ammonia could be reduced to nitrogen and hydrogen completing the pathway (NH_3➔N_2+H_2).

The computer simulation of NO reburning with a combination of CH_4/C_2H_2 showed promising results in terms of NO_x reduction. These findings were verified with the reburning experiments conducted later on in the project.

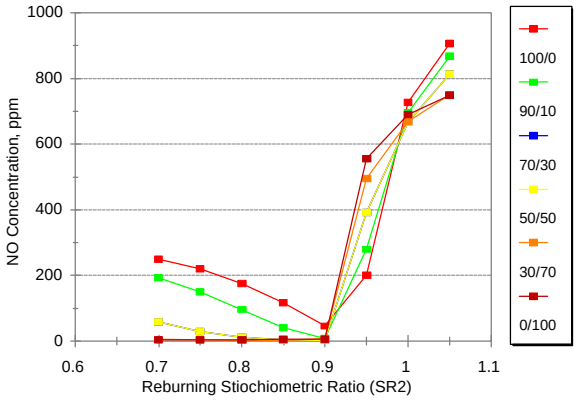

Figure 3.7 Effect of methane/acetylene composition on NO exit concentration in NO reburning (Input NO Concentration: 1000 ppm; Reactor Temperature: 1373 K; Residence Time: 0.2 s)

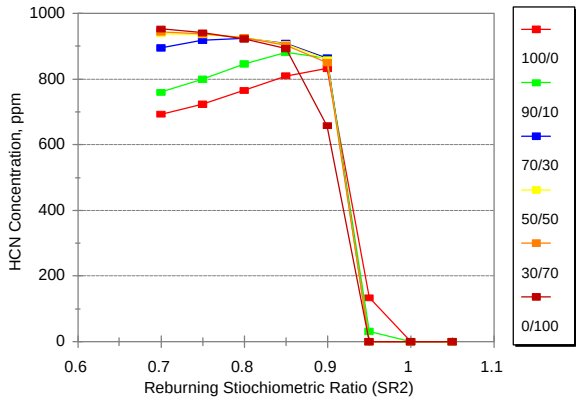

Figure 3.8 Effect of methane/acetylene composition on HCN exit concentration in NO reburning (Input NO Concentration: 1000 ppm; Reactor Temperature: 1373 K; Residence Time: 0.2 s)

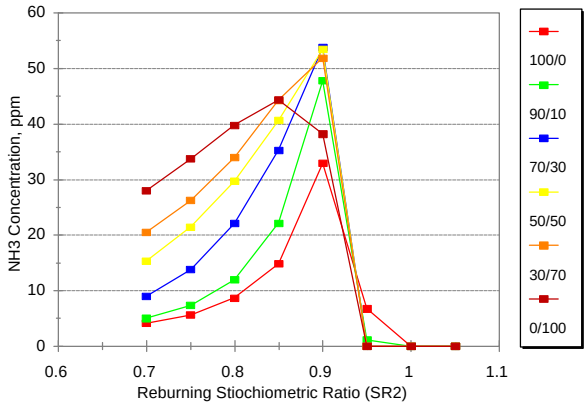

Figure 3.9 Effect of methane/acetylene composition on NH_3 exit concentration in NO reburning (Input NO Concentration: 1000 ppm; Reactor Temperature: 1373 K; Residence Time: 0.2 s)

3.5 Updated Reaction Mechanism

As many as 25 new reactions were added to the mechanism employed previously (218 reactions as presented in Table 3.1). Also, some of the reaction constants data was updated to improve the kinetics accuracy for the existing scheme. Listed in Table 3.2 is the updated version of the reaction mechanism.

Table 3.2 Updated reaction mechanism

REACTIONS CONSIDERED	(k = A T**b exp(-E/RT)) A	b	E
1. C2H6+M=2CH3+M	5.80E+13	0.0	75000.0
2. CH4+M=CH3+H+M	4.17E+17	0.0	92300.0
H2O Enhanced by 5			
3. CH4+O2=CH3+HO2	4.00E+13	0.0	56910.0
4. CH4+H=CH3+H2	2.02E+04	3.0	8750.0
5. CH4+OH=CH3+H2O	1.90E+05	2.4	2110.0
6. CH4+O=CH3+OH	1.02E+09	1.5	8604.0
7. CH4+HO2=CH3+H2O2	1.80E+11	0.0	18700.0
8. CH4+CH2=CH3+CH3	4.30E+13	0.0	10030.0
9. CH3+CH2O=CH4+HCO	5.50E+03	2.8	5860.0
10. CH3+HCO=CH4+CO	1.20E+14	0.0	0.0
11. CH3+M=CH2+H+M	1.90E+16	0.0	91600.0
12. CH3+HO2=CH3O+OH	2.00E+13	0.0	0.0
13. CH3+O2=CH3O+O	2.05E+19	-1.6	29229.0
14. CH3+O=CH2O+H	8.40E+13	0.0	0.0
15. CH3+OH=CH2+H2O	7.50E+06	2.0	5000.0
16. CH3+H=CH2+H2	9.00E+13	0.0	15100.0
17. CH3O+M=CH2O+H+M	1.00E+14	0.0	25000.0
18. CH2OH+M=CH2O+H+M	1.00E+14	0.0	25000.0
19. CH3O+H=CH2O+H2	2.00E+13	0.0	0.0
20. CH2OH+H=CH2O+H2	3.00E+13	0.0	0.0
21. CH3O+OH=CH2O+H2O	1.00E+13	0.0	0.0
22. CH2OH+OH=CH2O+H2O	1.00E+13	0.0	0.0
23. CH3O+O=CH2O+OH	1.00E+13	0.0	0.0
24. CH2OH+O=CH2O+OH	1.00E+13	0.0	0.0
25. CH3O+O2=CH2O+HO2	6.30E+10	0.0	2600.0
26. CH2OH+O2=CH2O+HO2	1.48E+13	0.0	1500.0
27. CH2+HCO=CH3+CO	2.00E+13	0.0	0.0

28. CH2+H=CH+H2	1.00E+17	-1.2	0.0
29. CH2+OH=CH+H2O	1.13E+07	2.0	3000.0
30. CH2+OH=CH2O+H	3.00E+13	0.0	0.0
31. CH+O2=HCO+O	3.30E+13	0.0	0.0
32. CH+O=CO+H	1.00E+13	0.3	0.0
33. CH+OH=HCO+H	5.00E+13	0.0	0.0
34. CH+CO2=HCO+CO	3.40E+12	0.0	690.0
35. CH+H=C+H2	1.50E+14	0.0	0.0
36. CH+H2O=CH2O+H	5.70E+12	0.0	-755.0
37. CH+CH2O=CH2CO+H	9.46E+13	0.0	-515.0
38. CH+C2H2=C3H2+H	8.40E+13	0.0	0.0
39. CH+CH2=C2H2+H	4.00E+13	0.0	0.0
40. CH+CH3=C2H3+H	3.00E+13	0.0	0.0
41. CH+CH4=C2H4+H	6.00E+13	0.0	0.0
42. C+O2=CO+O	2.00E+13	0.0	0.0
43. C+OH=CO+H	5.00E+13	0.0	0.0
44. C+CH3=C2H2+H	5.00E+13	0.0	0.0
45. C+CH2=C2H+H	5.00E+13	0.0	0.0
46. CH2+CO2=CH2O+CO	1.10E+11	0.0	1000.0
47. CH2+O=CO+2H	1.70E+13	0.2	0.0
48. CH2+O=CO+H2	9.00E+12	0.2	0.0
49. CH2+O2=CO2+2H	1.60E+12	0.0	1000.0
50. CH2+O2=CH2O+O	5.00E+13	0.0	9000.0
51. CH2+O2=CO2+H2	6.90E+11	0.0	500.0
52. CH2+O2=CO+H2O	1.90E+10	0.0	-1000.0
53. CH2+O2=CO+OH+H	8.60E+10	0.0	-500.0
54. CH2+O2=HCO+OH	4.30E+10	0.0	-500.0
55. CH2O+M=CO+H2+M	8.30E+15	0.0	69550.0
56. CH2O+O=CO2+2H	3.50E+05	2.4	1360.0
57. CH2O+OH=HCO+H2O	3.43E+09	1.2	-447.0
58. CH2O+H=HCO+H2	2.19E+08	1.8	3000.0
59. CH2O+M=HCO+H+M	1.00E+16	0.0	80270.0
60. CH2O+O=HCO+OH	1.70E+16	2.3	3080.0
61. HCO+OH=H2O+CO	1.00E+14	0.0	0.0
62. HCO+H=CO+H2	1.19E+13	0.3	0.0
63. HCO+O=CO+OH	3.00E+13	0.0	0.0
64. HCO+O=CO2+H	3.00E+13	0.0	0.0
65. HCO+O2=HO2+CO	3.30E+13	-0.4	0.0
66. CO+O+M=CO2+M	6.17E+14	0.0	3000.0
67. CO+OH=CO2+H	1.51E+07	1.3	-758.0
68. CO+O2=CO2+O	2.50E+12	0.0	47700.0
69. HO2+CO=CO2+OH	5.80E+13	0.0	22934.0
70. C2H6+CH3=C2H5+CH4	5.50E-01	4.0	8300.0

71. C2H6+H=C2H5+H2	5.40E+02	3.5	5210.0
72. C2H6+O=C2H5+OH	1.20E+12	0.6	7310.0
73. C2H6+OH=C2H5+H2O	8.70E+09	1.0	1810.0
74. C2H4+OH=CH2O+CH3	5.60E+12	0.0	1500.0
75. C2H4+CH3=C2H3+CH4	6.60E+00	3.7	9500.0
76. C2H4+H=C2H3+H2	1.30E+06	2.5	12240.0
77. C2H4+OH=C2H3+H2O	9.00E+13	0.0	6860.0
78. CH2+CH3=C2H4+H	4.20E+13	0.0	0.0
79. C2H5+M=C2H4+H+M	1.00E+17	0.0	31000.0
80. C2H5+H=2CH3	2.30E+12	0.5	0.0
81. C2H5+O2=C2H4+HO2	8.43E+11	0.0	3875.0
82. C2H2+O=CH2+CO	1.70E+08	1.6	2210.0
83. C2H2+O=HCCO+H	2.50E+08	1.6	2210.0
84. H2+C2H=C2H2+H	4.09E+05	2.4	864.0
85. C2H3+M=C2H2+H+M	8.00E+14	0.0	31550.0
86. C2H3+H=C2H2+H2	4.00E+13	0.0	0.0
87. C2H3+O=CH2CO+H	3.30E+13	0.0	0.0
88. C2H3+O2=C2H2+HO2	4.00E+12	0.0	-250.0
89. C2H3+OH=C2H2+H2O	5.00E+12	0.0	0.0
90. OH+C2H2=C2H+H2O	3.37E+07	2.0	14000.0
91. OH+C2H2=CH2CO+H	2.18E-04	4.5	-1000.0
92. CH2CO+H=CH3+CO	1.13E+13	0.0	3428.0
93. CH2CO+H=HCCO+H2	5.00E+13	0.0	8000.0
94. CH2CO+O=HCCO+OH	1.00E+13	0.0	8000.0
95. CH2CO+O=CH2O+CO	1.50E+12	0.0	1350.0
96. CH2CO+OH=HCCO+H2O	7.50E+12	0.0	3000.0
97. CH2CO+M=CH2+CO+M	1.50E+15	0.0	57600.0
98. C2H+O2=CO+HCO	5.00E+13	0.0	1500.0
99. C2H+C2H2=C4H2+H	4.00E+13	0.0	0.0
100. O+HCCO=H+2CO	1.00E+14	0.0	0.0
101. HCCO+O2=2CO+OH	1.60E+12	0.0	854.0
102. CH+HCCO=C2H2+CO	5.00E+13	0.0	0.0
103. 2HCCO=C2H2+2CO	1.00E+13	0.0	0.0
104. C2H+O=CH+CO	5.00E+13	0.0	0.0
105. C2H+OH=HCCO+H	2.00E+13	0.0	0.0
106. 2CH2=C2H2+2H	1.00E+12	0.6	0.0
107. CH2+HCCO=C2H3+CO	3.00E+13	0.0	0.0
108. C4H2+OH=C3H2+HCO	3.00E+13	0.0	0.0
109. C3H2+O2=HCO+HCCO	1.00E+13	0.0	0.0
110. C4H2+O=C3H2+CO	2.70E+13	0.0	1700.0
111. C2H2+M=C2H+H+M	4.20E+16	0.0	107000.0
112. C2H4+M=C2H2+H2+M	1.50E+15	0.0	55440.0
113. C2H4+M=C2H3+H+M	1.40E+16	0.0	81280.0

114. H2+O2=2OH		1.70E+13	0.0	47780.0
115. OH+H2=H2O+H		6.40E+06	2.0	2961.0
116. O+OH=O2+H		4.50E+14	-0.5	600.0
117. O+H2=OH+H		5.06E+04	2.7	6290.0
118. H+O2+M=HO2+M		7.00E+17	-0.8	0.0
H2O	Enhanced by 18.6			
CO2	Enhanced by 4.2			
H2	Enhanced by 2.86			
CO	Enhanced by 2.11			
N2	Enhanced by 1.26			
119. H+HO2=2OH		2.50E+14	0.0	1900.0
120. O+HO2=OH+O2		4.80E+13	0.0	1000.0
121. OH+HO2=H2O+O2		5.00E+13	0.0	1000.0
122. 2OH=O+H2O		2.10E+08	1.4	-400.0
123. 2H+M=H2+M		1.00E+18	-1.0	0.0
H2	Enhanced by 0			
H2O	Enhanced by 0			
CO2	Enhanced by 0			
124. 2H+H2=2H2		9.20E+16	-0.6	0.0
125. 2H+H2O=H2+H2O		6.00E+19	-1.3	0.0
126. 2H+CO2=H2+CO2		5.49E+20	-2.0	0.0
127. H+OH+M=H2O+M		7.50E+23	-2.6	0.0
H2O	Enhanced by 5			
128. 2O+M=O2+M		1.89E+13	0.0	-1788.0
129. H+HO2=H2+O2		2.50E+13	0.0	700.0
130. 2HO2=H2O2+O2		2.00E+12	0.0	0.0
131. H2O2+M=2OH+M		1.20E+17	0.0	45500.0
132. H2O2+H=HO2+H2		1.70E+12	0.0	3750.0
133. H2O2+O=HO2+OH		9.60E+06	2.0	3974.0
134. H2O2+OH=H2O+HO2		1.00E+13	0.0	1800.0
135. CH+N2=HCN+N		3.00E+11	0.0	13600.0
136. CN+N=C+N2		1.90E+15	-0.6	0.0
137. CH2+N2=HCN+NH		1.00E+13	0.0	74000.0
138. H2CN+M=HCN+H+M		3.00E+14	0.0	22000.0
139. C+NO=CN+O		3.70E+13	0.0	0.0
140. CH+NO=HCN+O		1.10E+14	0.0	0.0
141. CH2+NO=HCNO+H		1.39E+12	0.0	-1100.0
142. CH3+NO=HCN+H2O		5.30E+11	0.0	15000.0
143. CH3+NO=H2CN+OH		5.30E+11	0.0	15000.0
144. HCCO+NO=HCNO+CO		2.00E+13	0.0	0.0
145. HCNO+H=HCN+OH		1.00E+14	0.0	12000.0
146. HNCO+O=NCO+OH		2.00E+06	2.1	11415.0
147. HNCO+OH=NCO+H2O		6.40E+05	2.0	2560.0

148. CH2+N=HCN+H	5.00E+13	0.0	0.0
149. CH+N=CN+H	1.30E+13	0.0	0.0
150. CO2+N=NO+CO	1.90E+11	0.0	3400.0
151. HCCO+N=HCN+CO	5.00E+13	0.0	0.0
152. CH3+N=H2CN+H	3.00E+13	0.0	0.0
153. C2H3+N=HCN+CH2	2.00E+13	0.0	0.0
154. HCN+OH=CN+H2O	1.45E+13	0.0	10929.0
155. OH+HCN=HOCN+H	5.85E+04	2.4	12500.0
156. OH+HCN=HNCO+H	1.98E-03	4.0	1000.0
157. OH+HCN=NH2+CO	7.83E-03	4.0	4000.0
158. HOCN+H=HNCO+H	1.00E+13	0.0	0.0
159. HCN+O=NCO+H	1.38E+04	2.6	4980.0
160. HCN+O=NH+CO	3.45E+03	2.6	4980.0
161. HCN+O=CN+OH	2.70E+09	1.6	29200.0
162. CN+H2=HCN+H	2.95E+05	2.5	2237.0
163. CN+O=CO+N	1.80E+13	0.0	0.0
164. CN+O2=NCO+O	7.50E+12	0.0	-389.0
165. CN+OH=NCO+H	6.00E+13	0.0	0.0
166. HO2+NO=NO2+OH	2.11E+12	0.0	-479.0
167. NO2+H=NO+OH	3.50E+14	0.0	1500.0
168. NO2+O=NO+O2	1.00E+13	0.0	600.0
169. NO2+M=NO+O+M	7.30E+14	0.0	53000.0
170. NCO+H=NH+CO	5.00E+13	0.0	0.0
171. NCO+O=NO+CO	4.70E+13	0.0	0.0
172. NCO+N=N2+CO	2.00E+13	0.0	0.0
173. NCO+OH=NO+CO+H	1.00E+13	0.0	0.0
174. NCO+M=N+CO+M	3.10E+16	-0.5	47700.0
175. NCO+NO=N2O+CO	6.20E+17	-1.7	763.0
176. NCO+H2=HNCO+H	7.60E+02	3.0	4000.0
177. HNCO+H=NH2+CO	2.20E+07	1.7	3800.0
178. NH+O2=HNO+O	1.00E+13	0.0	12000.0
179. NH+O2=NO+OH	1.00E+10	-0.2	4800.0
180. NH+O=NO+H	7.00E+10	0.0	0.0
181. NH+NO=N2O+H	2.90E+14	-0.4	0.0
182. N2O+OH=N2+HO2	2.00E+12	0.0	40000.0
183. N2O+H=N2+OH	3.30E+10	0.0	4729.0
184. N2O+M=N2+O+M	4.00E+14	0.0	56100.0
185. N2O+O=N2+O2	1.40E+12	0.0	10800.0
186. N2O+O=2NO	2.90E+13	0.0	23150.0
187. NH+OH=HNO+H	2.00E+13	0.0	0.0
188. NH+OH=N+H2O	5.00E+11	0.5	2000.0
189. NH+H=N+H2	1.00E+14	0.0	0.0
190. NH2+O=HNO+H	7.90E+14	-0.5	0.0

191. NH2+O=NH+OH	7.00E+12	0.0	0.0
192. NH2+OH=NH+H2O	4.00E+06	2.0	1000.0
193. NH2+H=NH+H2	6.92E+13	0.0	3650.0
194. NH2+NO=NNH+OH	1.39E+09	0.0	0.0
195. NH3+OH=NH2+H2O	2.04E+06	2.0	566.0
196. NH3+H=NH2+H2	6.36E+02	2.4	10171.0
197. NH3+M=NH2+H+M	1.40E+16	0.0	90600.0
198. NNH=N2+H	1.00E+04	0.0	0.0
199. NNH+NO=N2+HNO	5.00E+13	0.0	0.0
200. NNH+H=N2+H2	1.00E+14	0.0	0.0
201. NNH+OH=N2+H2O	5.00E+13	0.0	0.0
202. NNH+O=N2O+H	1.00E+14	0.0	0.0
203. HNO+M=H+NO+M	1.50E+16	0.0	48680.0
H2O Enhanced by 10			
O2 Enhanced by 2			
N2 Enhanced by 2			
H2 Enhanced by 2			
204. HNO+OH=NO+H2O	3.60E+13	0.0	0.0
205. HNO+H=H2+NO	5.00E+12	0.0	0.0
206. N+NO=N2+O	3.27E+12	0.3	0.0
207. N+O2=NO+O	6.40E+09	1.0	6280.0
208. N+OH=NO+H	3.80E+13	0.0	0.0
209. NO+NH2=N2O+H2	5.00E+13	0.0	24640.0
210. NO+N2H2=N2O+NH2	3.00E+12	0.0	0.0
211. NO2+NH2=N2O+H2O	1.90E+20	-3.0	0.0
212. HNO+NO=N2O+OH	2.00E+12	0.0	26000.0
213. HNO+HNO=N2O+H2O	4.00E+12	0.0	5000.0
214. N2O+CO=N2+CO2	5.00E+13	0.0	44000.0
215. HCCO+OH=HCO+CO+H	1.00E+13	0.0	0.0
216. HCO+M=CO+H+M	2.50E+14	0.0	16802.0
217. NH3+O=NH2+OH	2.10E+13	0.0	9000.0
218. NO+NH2=N2+H2O	2.00E+20	-2.6	925.0
219. NCO+O2=NO+CO2	2.00E+12	0.0	20000.0
220. NH+OH=NO+H2	2.00E+13	0.0	0.0
221. NH+NO=N2+OH	1.20E+15	-0.8	0.0
222. H+O+M=OH+M	4.70E+18	-1.0	0.0
223. HNCO+M=NH+CO+M	1.10E+16	0.0	86000.0
224. HNCO+O=NH+CO2	9.60E+07	1.4	8520.0
225. HNCO+O=HNO+CO	1.50E+08	1.6	44012.0
226. HNCO+HO2=NCO+H2O2	3.00E+11	0.0	29000.0
227. HNCO+O2=HNO+CO2	1.00E+12	0.0	35000.0
228. HNCO+NH2=NCO+NH3	5.00E+12	0.0	6200.0
229. HNCO+NH=NH2+NCO	3.00E+13	0.0	23700.0

230. NCO+OH=HCO+NO	5.00E+12	0.0	15000.0
231. NCO+HCO=HNCO+CO	3.60E+13	0.0	0.0
232. NCO+NO2=2NO+CO	1.30E+13	0.0	0.0
233. NCO+NO2=NO+NO+O2	5.40E+12	0.0	0.0
234. NCO+HNO=HNCO+NO	1.80E+13	0.0	0.0
235. NCO+HONO=HNCO+NO2	3.60E+12	0.0	0.0
236. NCO+NCO=2CO+N2	1.80E+13	0.0	0.0
237. NO2+NO2=2NO+O2	1.60E+12	0.0	26123.0
238. NO2+CO=NO+CO2	9.00E+13	0.0	33180.0
239. NO2+HCO=CO+HONO	2.10E+00	3.3	2350.0
240. NO2+HCO=NO+CO2+H	8.40E+15	-0.8	1930.0
241. HONO+H=NO2+H2	1.20E+13	0.0	7350.0
242. HONO+O=NO2+OH	1.20E+13	0.0	6000.0
243. HONO+OH=H2O+NO2	1.30E+10	1.0	135.0

NOTE: A units mole-cm-sec-K, E units cal/mole

Glarborg et al (1994) have carried out an experimental and theoretical study of isocyanic acid (HNCO) oxidation in an isothermal quartz flow reactor at 1 atm pressure in the temperature range 1025-1425 K. Due to its role as an important intermediate in fuel nitrogen oxidation , HNCO chemistry is important in our work as well. Reactions 223 through 243 listed in Table 3.2 are taken from the work of Glarborg et al (1994). These include HNCO paths (Miller and Bowman, 1991 and Miller and Melius, 1992) , NCO paths (Tsang, 1992) and HONO paths (Tsang, 1991). Efforts were made to include the most recent reaction constants data for reactions pertaining to NH_3 oxidation and the formation/ destruction of NO and N_2O. Reactions 182 through 186 include the recent reaction constants, taken from Davidson (1991) and Glarborg (1994). The new reaction constants data for R146 is from East (1993) and for R179 and R194 is from Linstedt (1994).

The reaction mechanism given in Table 3.2 is more comprehensive in terms of predicting the ammonia and isocyanic acid oxidation chemistry. However, this was first

employed to verify the accuracy of the already obtained CH_4/C_2H_2 reburning results before CH_4/NH_3 reburning studies were simulated.

Figures 3.10 through 3.12 compare the exit concentrations of NO, HCN and NH_3 at various reburning stoichiometric ratios for one reburn fuel composition, namely methane: 90% and acetylene: 10%. The impact of updating the reaction mechanism was not significant upon the NO reburning with a combination of methane and acetylene. The highest NO_x reduction occurs at SR2=0.9. Its important to note, however, that the reaction scheme needed changes to improve the accuracy of some reactions of crucial intermediates in methane/ ammonia reburning. An extensive literature survey was made in order to update the mechanism to the one listed in Table 3.2.

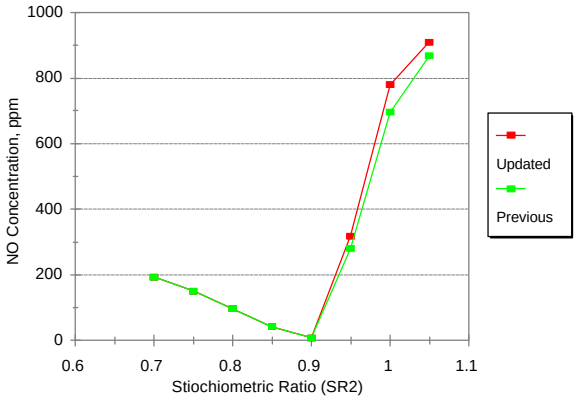

Figure 3.10 Comparison of the influence of the updated reaction mechanism over the previous reaction scheme on NO exit concentration in NO reburning with methane and acetylene as reburn fuel (90/10 composition)

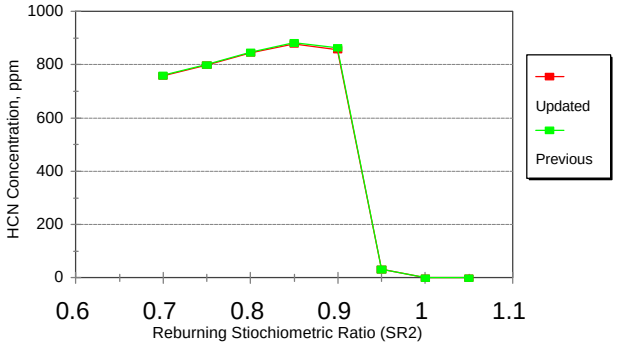

Figure 3.11 Comparison of the influence of the updated reaction mechanism over the previous reaction scheme on HCN exit concentration in NO reburning with methane/acetylene as reburn fuel (90/10 composition)

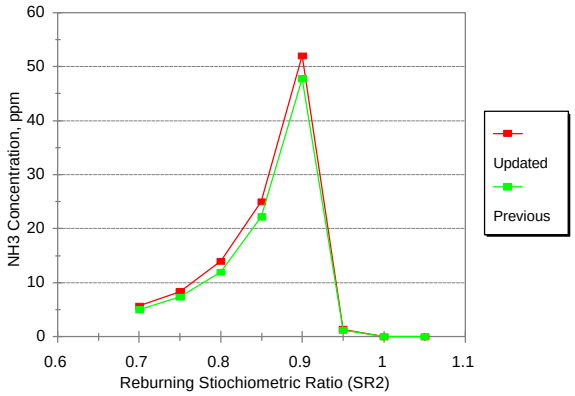

Figure 3.12 Comparison of the influence of the updated reaction mechanism over the previous reaction scheme on NH_3 exit concentration in NO reburning with methane/acetylene as reburn fuel (90/10 composition)

3.6 Results on NO Reburning with Methane and Ammonia

Computer modeling efforts were focussed then on NO reburning with a combination of methane and ammonia, the results of which are displayed in Figures 3.13 through 3.16. The updated reaction scheme was employed to run the CKINTERP program. Using the binary file created by executing the above program and the input SR2 conditions, the CHEMKIN package predicted the exit concentrations of various species involved in NO reburning. As in the case of methane/acetylene, the legends in Figures 3.13 through 3.16 describe the reburn fuel composition between methane and ammonia. A typical CH_4/NH_3: 96/4 combination at SR2=0.9 would represent the initial concentration of the flue gas as 2.11% CH_4, 0.0877% NH_3, 16.45% CO_2, 1.89% O_2, 1000 ppm NO and 79.366% N_2/He. The program was run for varying SR2 conditions for a fixed reburn composition and the entire process was repeated for various reburn fuel compositions. Unlike in the case of CH_4/C_2H_2, NO reburning with CH_4/NH_3 resulted in some N_2O formation. Figures 3.13 through 3.16 depict the exit concentrations of significant nitrogen containing species, namely NO, HCN, NH_3, N_2O for SR2 range of 0.7 to 1.05 and for various combinations of methane/ammonia. The residence time is 0.2 s and the reactor temperature is 1373 K for these runs.

From Fig. 3.13, it can be observed that the NO concentration has decreased considerably for 96/4 composition of CH_4/NH_3. This result looks very promising. The NO exit concentration for 100% methane reburning ranges 46-250 ppm while the composition

with 4% ammonia brings the concentration to 6-25 ppm. This can be a very significant reduction strategy.

Figure 3.14 shows that the HCN concentration drops considerably from 690-830 ppm range to 340-570 ppm range for SR2 values 0.7 to 0.9 with the introduction of 4% ammonia as reburn fuel. As mentioned earlier, HCN is highly unstable at high temperatures and its recovery is reported to be 30% at 1100 C for a residence time of 1 s (Song et al, 1982). From Fig. 3.15, we can observe an increase in ammonia concentration for the above SR2 range; the NH_3 concentration at SR2=0.9 is 157 ppm for CH_4/NH_3: 96/4 while it is 39 ppm for 100% CH_4 reburning. This level of exiting ammonia can be easily handled in the burnout zone where $NH_3+O_2 \rightarrow N_2+H_2O$. There is very little increase of N_2O at SR2=0.9 due to addition of ammonia in the reburn fuel, as seen in Fig. 3.16.

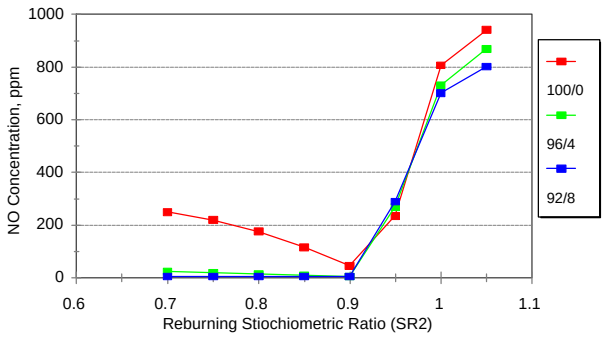

Figure 3.13 Effect of methane/ammonia composition on NO exit concentration in NO reburning (Input NO Concentration: 1000 ppm; Reactor Temperature: 1373 K; Residence Time: 0.2 s)

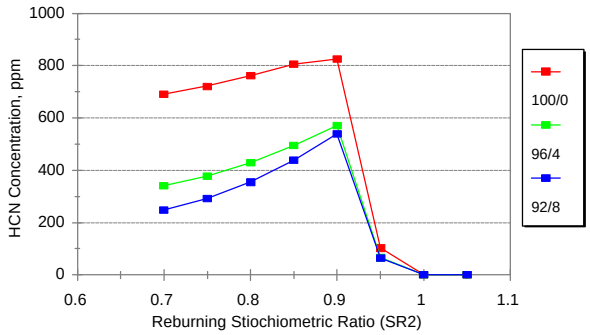

Figure 3.14 Effect of methane/ammonia composition on HCN exit concentration in NO reburning (Input NO Concentration: 1000 ppm; Reactor Temperature: 1373 K; Residence Time: 0.2 s)

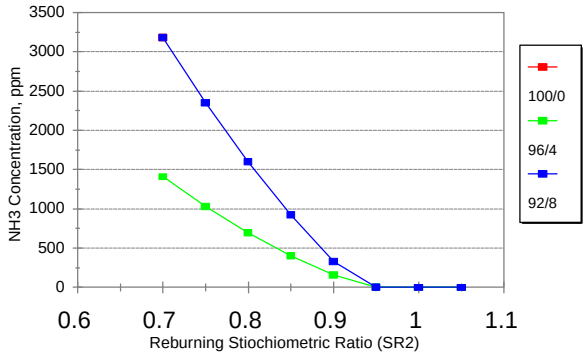

Figure 3.15 Effect of methane/ammonia composition on NH_3 exit concentration in NO reburning (Input NO Concentration: 1000 ppm; Reactor Temperature: 1373 K; Residence Time: 0.2 s)

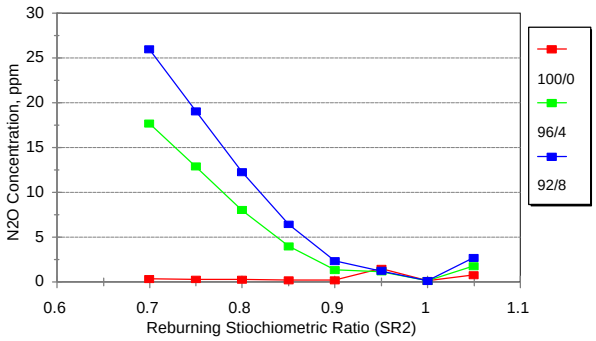

Figure 3.16 Effect of methane/ammonia composition on N_2O exit concentration in NO reburning (Input NO Concentration: 1000 ppm; Reactor Temperature: 1373 K; Residence Time: 0.2 s)

3.7 Summary

On the whole for 96% methane and 4% ammonia, the best operating point will be SR2=0.9. Comparing its effect with 100% methane as reburn fuel, the NO concentration reduced from 46 ppm to 6 ppm out of the initially fed 1000 ppm. While HCN concentration reduced from 830 ppm to 570 ppm, ammonia concentration increased from 40 ppm to 160 ppm. This trend could be due to trace amounts of unreacted ammonia slippage through the reburning zone. Also, the reduction seen in HCN could have reflected on ammonia increase through the series reaction NO→HCN→NH_3. The increase in N_2O is negligible (0.24 ppm to 1.33 ppm) and is well within the state and federal limits.

On the whole for 90% methane and 10% acetylene the best operating point will be SR2=0.9 as well. Comparing with the results of 100% methane reburning, the NO concentration has decreased from 46 ppm to 7 ppm from the initially fed 1000 ppm; the HCN

concentration increased slightly from 833 ppm to 864 ppm and the NH_3 increased from 33 ppm to 47 ppm. Considering the high instability at high temperatures and the burnout zone reactions the HCN could be easily handled. Likewise, ammonia will be converted to nitrogen and water in the burnout zone and hence would not be a problem. The N_2O level is practically insignificant for both cases, either 100 % methane or 90% methane/ 10% acetylene.

The above observations would point to the fact that the presence of ammonia almost brings NO→HCN to completion and at the same time greatly favors HCN→NH_3. That is why we see a little more ammonia formation and less HCN concentration. The presence of 10% acetylene greatly favors the completion of NO→HCN but favors the HCN →NH_3 very little. That is why we observe increased HCN concentration and insignificant increase in ammonia concentration.

The above findings led us to the experimental and these predictions/trends were subsequently verified at the experimental facility, designed and built on the Rust College campus under this grant instrument.

Chapter IV

EXPERIMENTAL DESIGN AND TESTING FACILITY

Technical discussions with the then project officer Dr. Lori Gould and Mr. James Ekmann at Pittsburgh Center coupled with the preliminary computer predictions guided the research team to carefully design the experimental work under this grant instrument. This chapter focuses on the experimental design and testing facility. Chapter V presents the results of the experimental studies undertaken as a result of careful and thoughtful planning by the research team and the DOE personnel.

4.1 Choice of Reactor

Many experimental techniques including shock tubes, stirred reactors, turbulent reactors have been considered. Because of physical equipment and processes involved, each of the above had its own merits and de-merits. Shock tubes are accurate with temperature and reaction time determinations but the actual reaction time achievable in a shock tube is very short (1 to 2.5 ms) compared to industrial furnaces. Also, in order to have consistent concentration, the analysis techniques require certain gas volume which may be a constraint with a shock tube. The stirred reactors have the merit of reaction getting to completion but strong back mixing will not be representative of the species found in an actual reburning situation. The actual reburning conditions can be met in large scale turbulent reactors since the dimensional and kinetic similarity can be maintained. However, there are lot of uncertainty factors such as (laminar or turbulent) nature of the flows, species concentration coupled with mixing influences and profiles of temperature which can not be properly defined

and hence meaningful analysis/conclusions can not be arrived at.

The reactor chosen for study is a plug flow tubular reactor, 1.885 cm ID, 65 cm length, assuming straight line velocity and temperature profiles. We chose to conduct experiments with the laminar flow reactor for the following reasons:

a) This reactor represents the actual reburning environments.

b) The experimental conditions are similar to actual industrial furnaces.

c) The low Reynolds number (20.6 < 2100; as shown in the reactor design, Section 4.2) ensures laminar flow; so, turbulent effects can be neglected.

d) The furnace can maintain the reaction temperature of 1100 C and it can reproduce the same temperature for subsequent experiments for comparison.

e) Other researchers have used some of the design practices proposed and have successfully carried out their experiments. For example,

I) Levy et al. (1981) used Helium as diluent gas; used temperatures of 1250-1750 K; used laminar flow tubular reactor; used similar coal (feeding) entrainment media and the same point of injection as ours.

ii) Chen et al. (1989) employed SR1=1.1; used residence time of 0.4 s; used gas washing method and specific ion electrodes to measure HCN and NH_3 species.

The gases from cylinders are metered through rotameters and mixed in the buffer chamber so that the gas mixture represents the flue gas from the primary combustion zone, characterized by stoichiometric ratio SR1. Then the gaseous mixture is passed through the reactor where reburning fuel is injected and the gaseous mixture would then be at the reburning stoichiometric ratio, SR2. The NO from combustion zone will be reduced to N_2

and CO_2 through a series of chemical reactions (250 odd reactions). Using this reactor, we developed data such as NO_x reduction by reburning with methane, a combination of methane and acetylene and non-selective catalytic reduction with ammonia and conducted a host of other heterogeneous combustion tests.

To prove the device yields information of desired quality, we first tested if CH_4 reburning resulted in similar NO reduction, as reported by previous researchers and upon confirmation only, we proceeded to other tests planned under this grant instrument.

4.2 Reactor Design

Plug flow tubular ceramic reactor (1.885 cm I.D and 65 cm length, AD-998 alumina tube, Coors Ceramic).

Central portion of the reactor is enclosed in a 30 cm long, electrically heated laboratory tube furnace (Lyndberg Minimite Model 55035A).

SR2=0.9:

Gas	Volume Flow, cc/min	Density, g/cc	Weight, g/min
CO_2	321	0.0019768	6.35E-01
O_2	36.8	0.0014289	5.26E-02
N_2 /He	1549	1.769E-04	2.74E-01
NO	1.91	0.00134	2.56E-03
CH_4	41.7	7.167E-04	2.99E-02

Weight of the gas mixture, w_{mix} = 0.9936 g/min.

Average molecular weight of the mixture= $\sum$ (%vol (g-mole) * M.W.=11.392 g/g-mole

Mixture density (273 K, 1 atm)= Avg. M.W./Mol. Vol. =11.392/22.4E03= 5.086E-04 g/cc

Volumetric rate of the gas mixture at 273 K= w_{mix} /ρ_{mix} = 1954 cc/min.

Volumetric flow rate of the gas at 1100 C= 1954*1373/273 = 9826 cc/min.

A residence time of 0.2 seconds is typical for reburning zone. Therefore, the volume flow in 0.2 seconds is 9826*0.2/60 = 32.75 cc. For a tubular flow reactor, (π/4) $d^2 l$ = 32.75 cc. Assuming 1" O.D. and using Sch. 80 the inside diameter is 0.742", that is 1.885 cm. Therefore, the length of the reactor where T=1100 C is 32.75*4/(π*1.885^2)=11.74 cm.

Lyndberg assured that it could offer its model (55035 A) which has a reactor O.D. of 1" and it promised 1100 C for 12 cm length of reactor. So, we planned to use the above reactor with 55035A Lyndberg Minimite furnace.

Central portion of the reactor surrounded by the furnace:

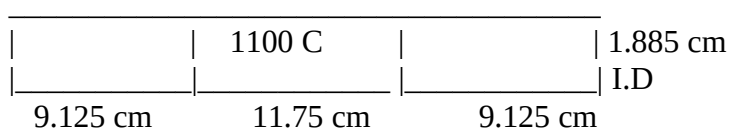

Lyndberg Minimite furnace keeps the 11.75 cm of heated length at 1100 C.

Mention must be made that our experiments were performed with gas in the reactor at 1100 C and we ensured the feasibility by buying a 1200 C Thermolyne tube furnace (F21135) in stead of a 1100 C Minimite furnace while purchasing the furnace. This Thermolyne tube furnace was purchased from Pacific Combustion Engineering Company. This furnace has one set point control in the middle portion of the process tube (made of mullite) that maintained a temperature upto 1200 ± 5 C for a length of 10 cm.

Residence time calculation in the heating zone of the reactor

From the reactor design calculations, we find the volume rate of the gas mixture as 9826 cc/min at 1100 C. For a given reactor cross-sectional area, this would mean 9826/ $(\pi/4)1.885^2$ = 3521 cm/min of linear velocity. To cover 9.125 cm of reactor length, it would take 9.125*60/3521 =0.1555 s. The heating time of 0.0477 s (See rate of gas heating calculations, Section 4.3) is < 0.1555 s. So the gas can easily get heated to 1373 K.

Reynolds Number

Volumetric flow of gas at 1100 C (as in the previous section), V= 9826 cc/min

Cross-sectional Area of the reactor tube, A= $\pi/4$ (1.885E-02)^2 m^2

Velocity, v = V/A = 35.21 m/min = 58.68 cm/s

Density of the gas mixture at 1100 C, $\rho_{mix} = w_{mix} / V_{mix}$ =0.9936/9826= 1.011E-04 g/cc

At SR2=0.9

Gas	Percent Composition, x %	Absolute Viscosity,μ g/m-sec
Carbon Dioxide	16.45	0.057
Oxygen	1.89	0.061
Helium	79.43	0.054
Nitric Oxide	0.1	0.054
Methane	2.14	0.038

Viscosity of the mixture, $\mu_{mix} = \sum x\mu / \sum x$ = 5.43E-02 g/m-sec

Since the species are all in the gas phase, the viscosities of which are very negligible (μ_{mix} =0.00543 g/m-s), we will ignore any wall effects, since it is also going to be negligible.

Reynolds Number, Re = D v ρ_{mix} / μ_{mix} = 20.6

Since Re < 2100 for a flow of a fluid through a circular tube, we can conclude that the flow is laminar.

Mixing Chamber

The mixing chamber is just to prevent any surge inside the reactor and to create some back pressure in order to meter consistent and steady flow of various gases through various rotameters. The mixing chamber was made of stainless steel. The chamber was designed to provide 10 seconds of flow rate buffer capacity i.e 1950 cc/min*(10/60) =325 cc. Assuming 5 cm diameter, the length is 10 cm. This SS buffer tank was manufactured by M.K. Fabrication.

4.3 Rate of Gas Heating

Rate of gas heating calculations were performed using the radiative heat transfer to the gas mixture. However, another calculation was also performed based on pure convection since Mr. Ekmann insisted that the model not include radiation to verify whether the gas actually gets heated to the desired temperature within the time of its residence. Both methods yielded favorable result. The details are presented below.

4.3.1 Radiative heat transfer to the gas mixture

Heat gained by the gas mixture = Heat given by the radiative element (furnace walls)

$$mC_p dT = \sigma A \epsilon (T_w^4 - T^4) dt$$

Upon rearranging,

$$t = \frac{m}{\sigma A \epsilon} \int \frac{C_p dT}{T_w^4 - T^4}$$

where T_w is 1373 K and the integral limits are from 288 K (initial temperature of the gas mixture) to 1372 K (the temperature to which gas needs to be heated).

Also, mass of the mixture, m equals 2.26E-07 kg-mol (1 g/min divided by the M.W of the mixture, 11.4 times 0.1555 s/ 60 s times 1E-03 for kg/g conversion).

The Stefan-Boltzmann constant is 5.669E-08 $W/m^2/K^4$; emissivity of ceramic is 0.3 and surface area, A is given by π (.01885) (0.09125) m^2.

C_p of the gas mixture is 4.915+2.584E-03 T-1.6E-06 T^2 +3.92E-10 T^3 kcal/kg-mol/K

The integral now becomes:

$$\int \frac{C_p dT}{T_w^4 - T^4} = 4.915 \int \frac{dT}{T_w^4 - T^4} + 2.584E-03 \int \frac{T dT}{T_w^4 - T^4} - 1.6E-06 \int \frac{T^2 dT}{T_w^4 - T^4} + 3.92E-10 \int \frac{T^3 dT}{T_w^4 - T^4}$$

Upon integration this resolves to the following to which the integration limits (288 K to 1323 K or whichever T chosen) are to be applied.

$$4.915 * \frac{1}{4T_w^3} [\ln \frac{T_w + T}{T_w - T} + 2 \arctan \frac{T}{T_w}]$$

$$-1.6E-06 * \frac{1}{4T_w} [\ln \frac{T_w + T}{T_w - T} + 2 \arctan \frac{T}{T_w}]$$

$$+3.92E-10*-\frac{1}{4}\ln[T_w^4-T^4]$$

$$+2.584E-03*\frac{1}{4T_w^2}\ln\frac{T_w^2+T^2}{T_w^2-T^2}$$

Upon applying integration limits it is found that it takes 0.0477 seconds to heat the gas from 288 K to 1372 K which is very encouraging to the use of this particular reactor. Referring to the residence time calculation in the heating zone of the reactor (Section 4.2), it would take 0.1555 s for the gas at 1100 C to travel 9.125 cm moving at 59 cm/s. The time required to heat the gas from 288 K to 1372 K is 0.0477 s << 0.1555 s. So the gas will be at the appropriate temperature (1373 K) when it enters the reburning zone.

4.3.2 Heat transfer by convection

Question: Without radiation into account, for a laminar flow, what length of the tube is needed such that the exit bulk temperature of the gas is 1323 K? Take inlet temperature of the gas mixture as 273 K. The wall temperature is 1373 K (furnace temperature).

Velocity of the gas mixture, v= 0.5868 m/s

Diameter of the tube, d=0.01885 m

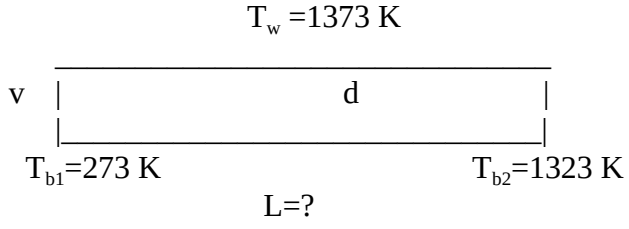

The heat transfer balance is given by

$$q = h\ \pi dL\ (T_w - \frac{T_{b1}+T_{b2}}{2}) = m\ c_p\ (T_{b2} - T_{b1})$$

Substituting temperatures and the diameter, this simplifies to:

$$31.09\ h\ L = 1050\ m\ c_p$$

The quantities m and c_p need to be calculated based on mean temperature ($T_{b,\ mean}$)=0.5(T_{b1}+T_{b2})= 798 K.

The composition of the gaseous mixture at SR2=0.9 along with various properties at 800 K is given below.

Gas	**% comp.**	**Density kg/m^3**	**Viscosity kg/m-s**	**Specific heat J/kg-C**	**thermal conductivity W/m-C**
CO_2	16.45	0.671	3.39 E-05	1126	0.0560
O_2	1.89	0.488	4.21 E-05	1054	0.0603
CH_4	2.14	0.2446	2.40 E-05	3936	0.1046
He	79.43	0.061	3.88 E-05	5197	0.3070
NO	0.1 (Negligible influence on the mixture properties)				
Mixture Properties		**0.07467**	**3.774E-05**	**4422.6**	**0.2567**

mass flow rate, m= ρ ($\pi d^2/4$) v= .07467* (π*.01885^2/4)*0.5868= 1.2228E-05 kg/s

The heat balance equation becomes upon substituting m and c_p:

$$h\ L = 1.8264\ W/m\text{-}C$$

Reynolds Number, Re_d = ρvd/μ= .07467*.5868*.01885/3.774E-05= 21.885

This confirms the laminar flow assumption.

Prandtl Number=$\mu c_p/k$=0.65

Peclet Number, Pe= $Re_d Pr$=14.225

Hausen has developed the following formula for the Nusselt Number (N_d) for fully developed laminar flow with constant wall temperature scenario which is valid for all ranges of Peclet Number*(d/L).

$$N_d = 3.66 + \frac{0.0668\ Pe\frac{d}{L}}{1+0.04\ (Pe\frac{d}{L})^{\frac{2}{3}}}$$

Since heat transfer coefficient, h is dependent on the length, L, let us choose a particular length, find h and calculate L based on the heat transfer balance equation, h L=1.8264. Reiterate the procedure until L converges to the actual length needed to heat the gas in the tube to the desired temperature.

Choose L=5 cm=0.05 m

Pe d/L = 14.225*0.01885/0.05 =5.363

Nu_d=3.979

h= $Nu_d k/d$=3.979*0.2567/0.01885=54.19 W/m^2-C

Therefore L=1.8264/h= 1.8264/54.19= 0.0337 m= 3.37 cm

Reiterate:

Pe d/L=7.9556 Nu_d=4.1184 h=56.08 W/m^2-C L=.0326 m =3.26 cm

Reiterate:

Pe d/L=8.2339 Nu_d=4.1329 h=56.28 W/m^2-C L=.03245 m =3.25 cm

We thus find that the length of the tubular reactor needed to heat the gas entering at a velocity

of 0.5868 m/s from 273 K to 1323 K, with wall temperature maintained at 1373 K is 3.25 cm. Also, the time taken to achieve this heating is very small (0.0325 m divided by 0.5868 m/s): 0.0553 s.

One of the key issues in the design was to make provision for measurement of gas temperature in the reactor at least after the gas has traversed the furnace length. In this way, we would measure the exit temperature of the gas, still in the reactor but outside the furnace portion. Hence the Coors ceramic reactor length of 65 cm was ideal to accommodate this measurement. A transition joint probe (TJ36-CAIN-316U-12) along with HH12 digital thermometer (thermocouple readout) for use in measuring the gas temperature in the reactor (exiting the furnace) were purchased from Omega Engineering. Due to the brittle nature of the ceramic reactor, both in terms of fixing end connections and with respect to accommodating thermocouple insertion, we sought the expertise of M.K Fabrication, which did an excellent job.

4.4 Other Design Concerns

a) Are catalytic effects probably negligible for PC firing?

Burch et al. (1991) reported that lignite, char, ash reduce NO from 1000 ppm to <50 ppm at pulverized coal combustion conditions. They reported also that lignite ash contains a major portion of CaO (28.2%), Barium (6570 ppm) and Strontium (4900 ppm). They suggested that these seem to be the most likely candidates for catalysts. The kind of reduction reported is not negligible and suggests that catalytic effects can be significant. Consequently in this work, surface catalyzed reburning has been shown to be a viable method to enhance

NO_x reduction by methane (Chapter V, Section 5.2.3).

b) Will the use of helium to adjust the heating rate, due to its lower thermal capacity, remove the study from realistic conditions?

Helium is used in this experiment for blending the gas (dilution) and to get the required flow rate of 1950 cc/min . The main reason helium is used is to minimize the heating time. Furthermore, helium similar to nitrogen is inert and hence will not remove the study from realistic conditions. As mentioned earlier, the simulated flue gas will consist of helium base producing rapid heating and cooling. Usually industries use 10% excess air to burn the coal completely. We assumed the same 10% excess O_2 and obtained the simulated flue gas composition: pure CO_2 - 327.67 cc/min, pure O_2 - 37.62 cc/min and NO- 1.95 cc/min. We assumed the primary zone fuel to be Pittsburgh coal. Upon our calculation, energy required to heat 1 kg-mol of gas mixture from 25 C to 1100 C with Helium as the diluent gas is 6585 kcal where as the heat required to do the same with N_2 as diluent gas is 8611 kcal. So, in order to heat the gas mixture with N_2 as diluent, we need 30% more heat energy and hence more heating time. Also, helium has been used as diluent gas by the following researchers, to cite a few.

I. Levy, J.M. , L.K. Chan, A.F.Sarofim and J.M.Beer (1981) and

ii. Singoredjo, L., F. Kapteijn, J.A. Moulijn and H.P. Boehm (1993).

4.5 NO_x Analyzer

The NO_x analyzer was purchased from California Analytical Instruments Inc. (Model 300 CLD). This measures 8 ranges of ppm from as low as 0-3 ppm range to as high as 0-30,000 ppm range. This utilizes the chemiilluminiscent method of determination of nitrogen oxides in a sample gas. The ultraviolet reaction of cylinder air produces molecular ozone, which in turn, converts the NO in the sample to NO_2 by gas phase oxidation. Typically, 10-15% of NO_2 molecules are elevated to an electronically excited state and reversion to a non-excited state results in emission of photons. The photons impinge on a photo diode detector that generates a DC voltage directly proportional to the NO contained in the sample gas. This current is amplified and presented to recorder output in ppm. For NO_x, the sample is routed to the NO_x converter where NO_2 is dissociated to NO and thereafter, the photo diode detector analyzes the sample.

4.6 Other Instruments of the Experimental Setup

Gas cylinders (He, O_2/He, CH_4/He, C_2H_2/He, CO_2, NH_3/He, NO/He) and corresponding **pressure regulators** were purchased from Mid-South Oxygen Company/ NexAir. The gas regulators for ammonia and NO cylinders must have non-corrosive passage and hence were to be made of stainless steel in stead of the commonly used brass. The team had to negotiate with various vendors on the prices of these items before making a final decision to go with the Mid-South Oxygen. All the cylinders were properly placed in chains and safety was ensured around the bench facility.

Flow meters for each gas (K-74 series rotameters) were purchased from King

Instrument Company. They were fixed to a panel and connected to a manifold through which the gas mixture was passed onto the buffer chamber.

Other supplies such as safety items, gas drying jar (drier) and desiccant (drierite) were purchased from Fisher Scientific; some of chemicals were purchased from Fisher while some others were bought from Aldrich; accessories such as ferrules, Teflon tubing were purchased from with McMaster Carr. The research team requested and received several coal samples for use from the DOE's Coal Samples Data Bank at PennState.

4.7 Testing Facility

Seven gas cylinders (He pure, 20.1% O_2/balance He, CO_2 pure, 20.1% CH_4/ balance He, 2.19% C_2H_2/ balance He, 0.352% NO/ balance He, 0.36% NH_3/ balance He), fitted with respective pressure regulators were placed in safety by a chain. The pressure regulators for ammonia and nitric oxide had to be stainless steel due the corrosive nature of the gases. A quarter inch teflon tubing was employed for all connections. Using the proper Swage-lok fittings and ferrules, the gas cylinders were connected to the inlet of respective flow meters. The flow meters employed were of K-74 series purchased from King Instrument Company. The ball valves for Oxygen and NO flow were made of stainless steel, the valves for CO_2 and helium were made of sapphire and the others were made of carboloy. All these were chosen to suit the desired flow rates through the respective flow meters. Figure 4.1 shows the front view of the panel on which the seven flow meters were fitted.

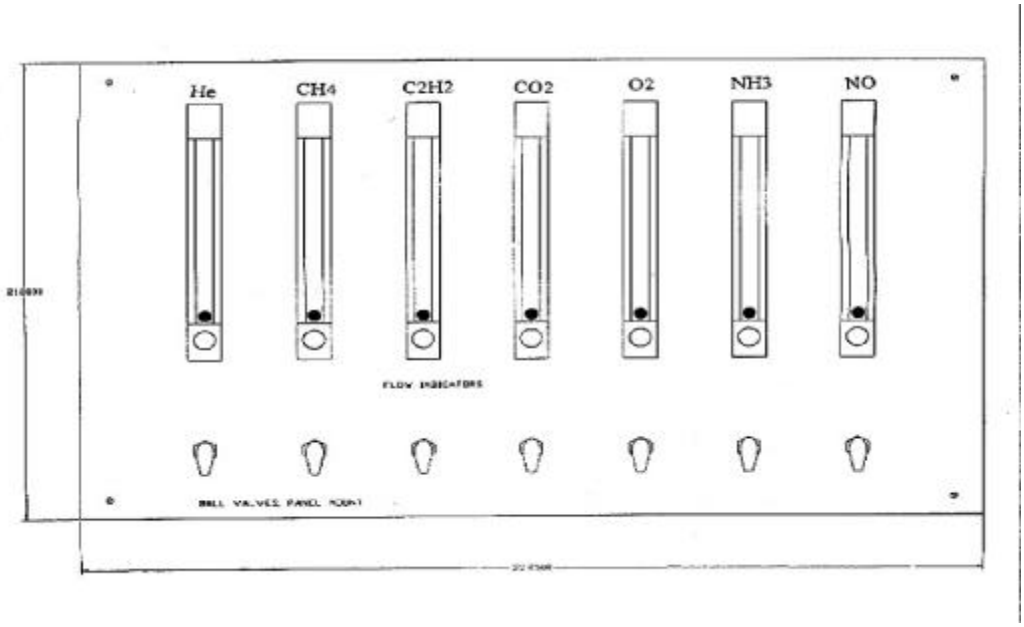

Figure 4.1 Front view of the panel mounted with flow meters

Figure 4.2 illustrates the process of mixing of the gases from the seven cylinders before the gas mixture enters the reactor. First, all the gases, upon leaving the respective flow meters enter into the stainless steel manifold. However, in order to ensure homogeneous mixing, the gas mixture is drawn into a stainless steel chamber from the manifold. This chamber acts as the buffer vessel where proper mixing takes place. Then the gas mixture is led to the reactor inlet through teflon tubing. Figure 4.3 shows the side view of the panel on which not only the flow meters but also the buffer vessel was mounted.

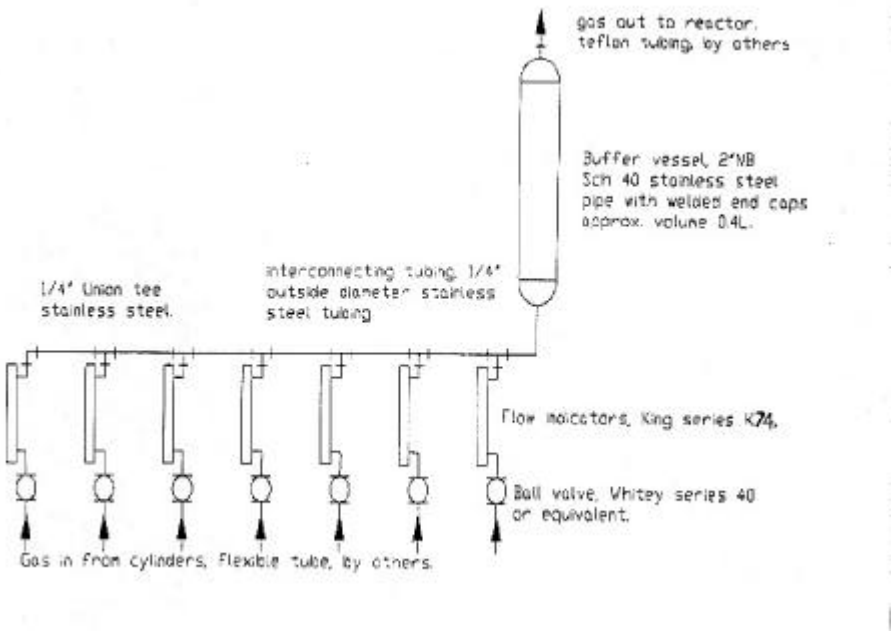

Figure 4.2 Schematic of gas flow through flow meters, manifold and buffer vessel

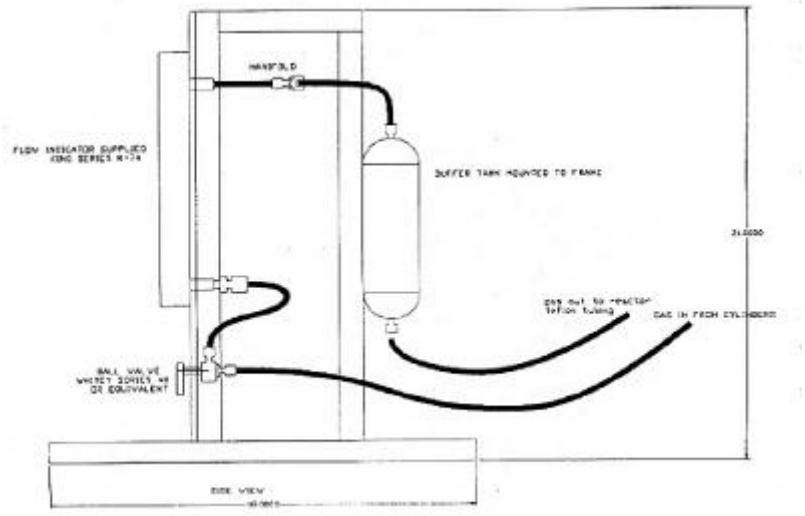

Figure 4.3 Side view of the panel showing flow meters, manifold and buffer vessel

The tubing is of 0.25" dia and the ceramic reactor is of 1" OD. Obviously we required ceramic tube adaptors on both ends of the reactor. Figure 4.4 shows the details of the inlet end adaptor. Notice the provision for coal injection. Upon finishing the reburning experiments with homogeneous gas mixture, we tested various coals as reburn fuel.

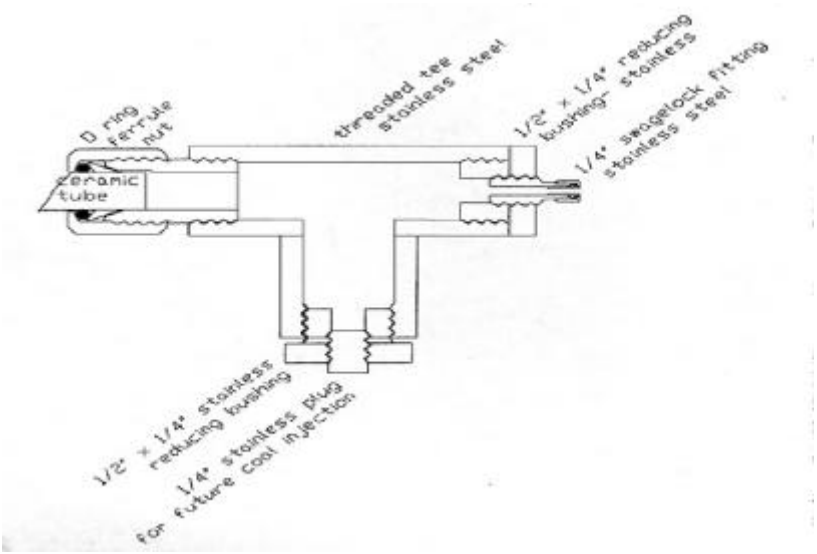

Figure 4.4 Ceramic reactor inlet end adaptor with leak proof connections

Figure 4.5 shows a similar adaptor for the exhaust end of the ceramic reactor. However, while one fitting was set for the gas flow, the other was adjusted for 3/16" thermocouple insertion. The Omega high temperature probe measured the gas temperature in the reactor about 3" inside the furnace. The ceramic reactor which is 26" long, was enclosed by a 1200 C Thermolyne furnace (15.5") in its middle portion. The reactor-furnace assembly was stationed horizontally for convenience during reburning with methane, acetylene and ammonia. It was held vertically for heterogeneous reactions with coal reburning. The temperature probe was connected to a HH12 digital thermometer.

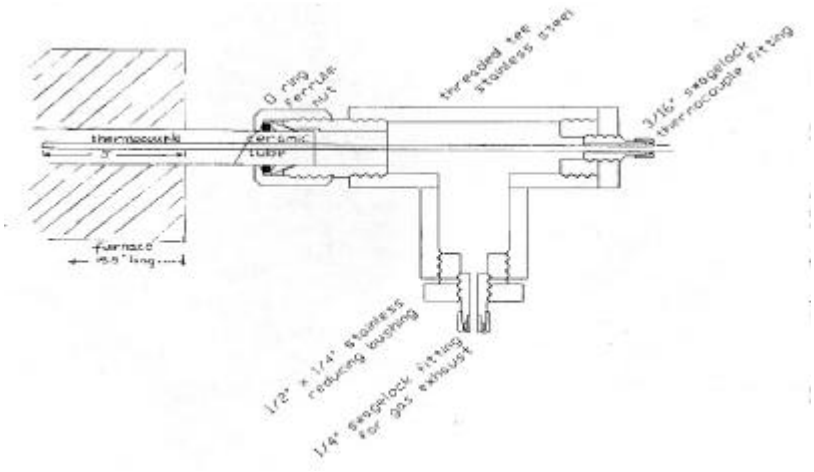

Figure 4.5 Ceramic reactor exhaust end adaptor with the thermocouple

The gas at the exhaust end of the reactor is led to the NO_x Analyzer via gas dryer. The dryer ensures removal of moisture. The tubing was ensured to be of sufficient length to cool the gas mixture to the temperature range acceptable for the operation of the analyzer. Remember, the analyzer is the costliest piece of equipment. The analyzer needs oxygen supply for the ozonator which is accommodated from the same oxygen cylinder used in the reburning experiments by employing a T connection. The gas, upon analysis, leaves the analyzer and vents through the exhaust of the building.

Certain changes were made in the design while building the coal feeder. Incorporating all the design requirements, the coal feeder and the feeding mechanism were constructed by M.K Fabrication. Presented herein are the details of the coal feeder and its operation.

4.8 Design and Operation of the Coal Feeder

The purpose of the coal feeder is to feed pulverized coal at low rates. A very practical coal feeder has been designed and documented by Burch et al. (1991b) to feed pulverized coal at a uniform feed rate. The uniform feeding is achieved by pneumatically stripping the coal particles. Following this design, we incorporated a variable speed motor to yield varying feed rates that accommodate smooth feeding of a variety of coal samples. The construction was done by M.K Fabrication. Upon receiving the coal feeder, we modified the reactor setup to have the coal feeder on a stand directly above the reactor to ensure proper passage of coal through the inside of the reactor.

The coal feeder essentially consists of 1/4" solid rod called as a piston and a 1/8" dia. Stainless steel tube locked together (to prevent deflection when the carriage mechanism moves up and down). This piston and feed tube is housed in a ½" dia. plexi-glass chamber. Coal is stored in this plexi-glass chamber. The glass chamber, in turn, is housed in 1" dia. SS tube with O-rings at the end to give a tight seal. The 1" SS tube is fixed onto a driving mechanism by means of a wing nut. This driving mechanism is moved up and down by a motor using a love-joy coupling. The polarity of the motor can be reversed to make it move up and down. As the driving mechanism moves up and down, the coal feeder attached to it will tend to follow the same course. In order for the gas connection in and out to the coal feeder not to get disconnected and in order to ensure uniform feeding of coal, the movement of coal feeder tube is arrested by a collar pin locked against solid bar of drive mechanism. This provides thrust for the piston rod and feed tube to slide against the SS tube housing through a Teflon ferrule. The Teflon ferrule allows movement of piston and feed tube as well

as provide leak tight connection at both ends of the coal feeder. The detailed features of the feeder and the feeding mechanism are shown in Figures 4.6 and 4.7. The parts are listed in Table 4.1.

Table 4.1. List of parts used in the building of the coal feeder and the coal feeding mechanism

key	part#	manufacturer	description
1	1A417	Dayton	shaft coupler body
2	4X176	Dayton	shaft coupler body
3	1X409	Dayton	shaft coupler insert
4		generic	½" stainless polished rod
5	2X567	Dayton	pillow block bearing
6	4X727	Dayton	center bearing
7		generic	piston 1/4" rod
8		generic	glass tube ½" od
9		generic	glass tube shield
10		generic	drive screw ½"x20 NC
11	2X568	Dayton	½" shaft collar
12	2X735	Dayton	1/4" shaft collar
13	4Z536	Dayton	gear motor
14	6A191	Dayton	speed controller
15		generic	switch 2 pole double throw
16		swagelock	½" Swagelock nut
17		swagelock	½" Swagelock connector
18		swagelock	½" Teflon ferrule
19		swagelock	½"x1/4" Swagelock reducer
20		swagelock	1/4" OD stainless tube
21		swagelock	½" Swagelock tee

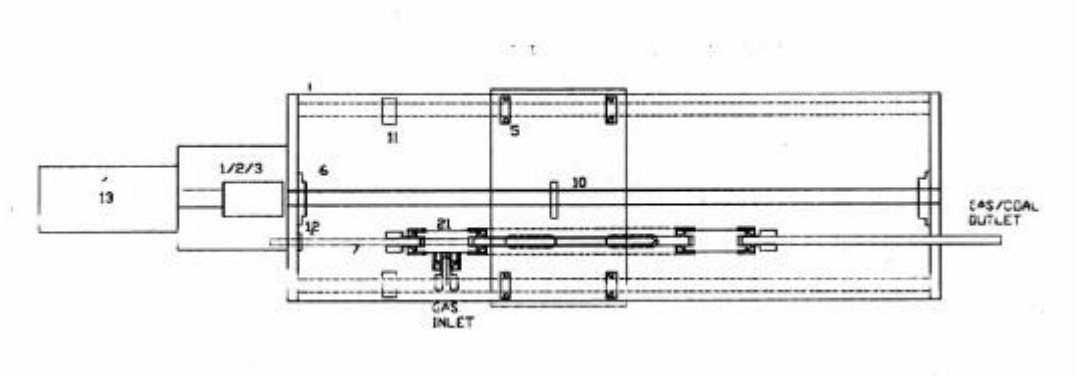

Figure 4.6 Coal injection general arrangement

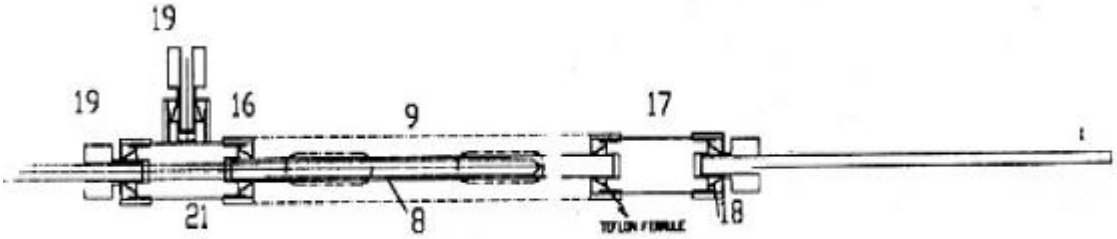

Figure 4.7 Coal feeder details

The gases such as He, CO_2 are allowed to enter the coal feeder at the top, strip the coal particles from the bed and feed it into the SS feed tube (1/8"). The coal particles have to be carefully ground to 40 microns to 200 microns, in order for the stripping to be effective. It is necessary that the coal bed is just below the feed hole in the feed tube at any point in time. The locked-in piston will not allow the feed tube to deflect.

Depending on the stoichiometry, the amperage to the motor is adjusted which in turn allows the motor to rotate at a specific speed. This in turn rotates the driving mechanism which in turn will try to move the coal feeder up. Since the coal feeder movement is restricted by the collar pin, it thereby drives the coal feeder housing, up the piston and the feed tube. So the movement of the piston should be exactly equal to the rate at which the coal is fed in order to maintain the feed tube's hole just right above the coal bed. Various feed stoichiometry can be achieved by driving the coal feeder mechanism accordingly and by maintaining necessary gas feed enough to cause coal particle stripping.

4.9 Challenges

The entire experimental activity was challenging for the research team. Just when the coal feeder begins to do what it is supposed to do, the analyzer wouldn't operate properly. The U-V lamp (ozone lamp) in the NO_x analyzer failed time and again despite all the care we have taken to comply with the conditions under which the analyzer must be operated. The manufacturer (California Analytical Instruments) introduced a new style U-V lamp that allowed for greater ozone output and hoped that failures may not reoccur. It turned out that the circuit boards designed could not function well with the new style lamp; the blow-out occurred in less than two hours due to excessive heat. The manufacturer reverted to previous style ozonator setup and believed that the analyzer would function properly. At times, the work was greatly hampered and yet, we persisted with the research patiently working with the manufacturer in getting the analyzer repaired whenever we needed. In the personal opinion of the PI, while he appreciates the manufacturer for the repair work, he would not

suggest other DOE researchers to purchase analyzers from this manufacturer.

The attempt to vary the coal feeding rate was limited by the length of the solid piston rod and in time the piston rod was replaced. However, it was observed that the coal feeder was not feeding properly. Seeing the bending of the feeder, it was decided to drill larger holes at both ends of the carriage mechanism where the coal feeder is mounted. The wing nut would still do the locking. It seemed to work well preventing deflection when the carriage mechanism moved up and down. Soon came the problem of broken plexi-glass chamber in which the piston and the feed tube are housed. Two pieces of the plexi-glass chamber were purchased through M.K Fabrication. Assembling the coal feeder mechanism again, the coal feeder was tested for its operation. The motor was turned on and rotation was observed at the love-joy coupling but the driving mechanism was not moving up and down. Expecting the coupler inserts were not acting properly, they were replaced and the feeder mechanism was tested. Even the collar shaft was replaced. After a lot of trials to fix the coal feeder mechanism, it was determined that the coal feeder had a defective part only the builder could repair. The nut fitting had been malfunctioning and the threaded shaft moving the coal feeder mechanism up and down was getting deformed. Hence the coal feeder was not feeding properly. The feeder was fixed by M.K Fabrication again and there were no more problems with its performance. Any problems with coal stripping were solved by adding silica gel to the coal/catalyst particles. Such challenges are always the teaching tools in research and these are presented to benefit the research community in general.

The next chapter details the experimental studies conducted and the pertinent results of those studies.

Chapter V

EXPERIMENTAL STUDIES

This chapter addresses the experimental results obtained at Rust College Test Facility described in detail in Chapter IV. At first, the NO_x reduction strategy involved reburning technology using the homogeneous, gas-phase reactions of NO with reburn fuels such as methane, acetylene and ammonia. The results pertaining to these homogeneous reactions are discussed in Section 5.1. Upon verifying the results with the computer simulation predictions (Chapter III), the research team set out to conduct heterogeneous reactions with various types of coal samples, char and surface catalysts, namely calcium carbide and calcium sulfide. These experiments involved reburning with coal, char gasification and surface catalyzed reburning the results of which are presented in Section 5.2. These results shed quite a lot of attraction for various methods as significant NO_x reduction technologies.

5.1 Homogeneous Reactions in NO_x Reduction

Discussed in this section are the results of various reburning tests, namely, NO reburning with methane, NO reburning with a combination of methane and acetylene and NO reburning with a combination of methane and ammonia.

5.1.1 Experimental results on NO reburning with methane

As many as 15 runs were conducted on nitric oxide reburning with methane. First, oxygen supply was initiated so as to allow flow into NO_x analyzer. While allowing the analyzer to warm up, the furnace was also turned on and with its temperature set point control, a particular furnace temperature was set. Slowly, helium and carbon dioxide cylinders were

opened and the flow levels calculated for a particular reburning stoichiometric ratio (SR2) were set. Similarly, the nitric oxide flow was adjusted so as to read 1000 ppm on the NO_x analyzer digital readout. The Omega probe measured the gas temperature inside the reactor which was read on the thermometer readout. When all the flow parameters were stable, methane was introduced according to the calculated flow rate for the particular SR2 in question. Instantly, the NO_x output decreased and once it reached a steady value, the reading was recorded. A constant check on gas leaks was crucial to the success of the experiment.

When the furnace temperature was set as 1130 C, the gas temperature 3" inside the reactor read 1092 C. The experiment was performed for five SR2 values, namely, 0.8, 0.85, 0.9, 0.95 and 1.0. The total flow rate of the gas mixture was 1950 cc/min. Given in Table 5.1 are the various flow rates of different gases for NO reburning with methane. Table 5.2 lists the actual flow rates, adjusted due to the varying gas proportions in the cylinders such as oxygen/He, methane/He and NO/He. These were calibrated for rotameter scales and fed into the flow meters. The steady readings on the NO_x analyzer before addition of methane and after addition of methane were recorded. The experimental results are shown in Table 5.3.

Table 5.1 Simulated flow rates of various gases for NO reburning with methane

SR2	CO_2	O_2	CH_4	NO	He
0.8	315.9	36.3	69.9	1.95	1526.0
0.85	318.4	36.8	55.1	1.95	1538.0
0.9	320.7	37.0	41.7	1.95	1548.9
0.95	322.7	37.3	29.6	1.95	1558.7
1.0	324.6	37.5	18.5	1.95	1567.7

Table 5.2 Adjusted flow rates due to varying gas proportions in the cylinders for NO reburning with methane

SR2	CO_2	O_2	CH_4	NO	He
0.8	315.9	180.4	347.6	553.4	1526.0
0.85	318.4	181.8	273.9	553.4	1538.0
0.9	320.7	183.1	207.4	553.4	1548.9
0.95	322.7	184.3	147.2	553.4	1558.7
1.0	324.6	185.4	92.2	553.4	1567.7

Later, the furnace temperature was adjusted to the maximum, that is, 1200 C which maintained the gas temperature as 1153 C. Five runs were conducted at this set temperature for the flow rates mentioned above (five SR2 conditions). Similar procedure was repeated for another temperature setting with furnace temperature of 1050 C and reaction temperature of 1010 C. All the results are summarized in Table 5.3.

Table 5.3 Experimental results on NO reburning with methane

Reburning SR2	Furnace T 1200 C Gas T 1153 C		Furnace T 1130 C Gas T 1092 C		Furnace T 1050 C Gas T 1010 C	
	NO in	NO out	NO in	NO out	NO in	NO out
0.8	998	5	1012	14	914	89
0.85	963	**3.7**	1018	10.3	922	72
0.9	960	**2**	1012	**6**	941	55
0.95	955	449	956	270	944	352
1.0	945	777	1018	852	1027	830

NO concentrations are measured in ppm.

It is apparent from Table 5.3 that the reburning stoichiometric ratio in the neighborhood of 0.9 is optimum for nitric oxide reduction and this result is agreeing with the predictions reported earlier in this research work (Chapter III). Similarly, the reaction temperature of about 1100 C as reported in the numerical simulation is verified to be optimum for NO reduction. The reduction at 1092 C as well as 1153 C is significant compared to reduction at 1010 C. In fact, these experimental results indicate better reduction than the predicted values; for example, a maximum reduction of 46 ppm was predicted at SR2=0.9 for NO reburning with methane at 1100 C while the experiment showed the NO reduction to be 6 ppm at 1092 C for the same SR2. These results are very encouraging for further investigation on reburning effectiveness of various fuels, in both homogeneous and heterogeneous reaction setting.

Extensive calculations were carried out on the reactor design (as shown in Chapter IV) to analytically verify the prediction that the gas will attain a temperature of 1100 C inside the reactor. It was experimentally verified during NO reburning with methane, as already pointed out earlier and shown in Table 5.3. The gas temperature inside the reactor measured 3" inside the furnace (or approximately 5" from the center of the furnace length) is about 40-50 C lower. Hence, the gas temperature could even be only 20 C lower at the middle portion of the furnace/reactor. The measurement of gas temperature served as an important tool in establishing the proper reaction conditions in nitric oxide reburning.

5.1.2 Experimental results on NO reburning with methane/ acetylene

Presented herein are the experimental results of NO reburning with methane/acetylene. The results are consistent with model predictions presented in Chapter III. The experimental procedure employed for nitric oxide reburning with methane/acetylene was very similar to the one employed for reburning with methane. First, the furnace was turned on and with its temperature set point control, a furnace temperature in the neighborhood of 1140 C was set. Slowly, helium, oxygen and carbon dioxide cylinders were opened and the flow levels calculated for a particular reburning stoichiometric ratio (SR2) were set. Oxygen simultaneously flowed through the NOx analyzer. The analyzer was turned on and allowed to warm up. The parameters on the analyzer were checked until they reached the normal operating conditions. Then, the nitric oxide flow was adjusted to 1000 ppm which was expressed on the NOx analyzer digital readout. The Omega probe measured the gas temperature inside the reactor which was digitized on the thermometer readout. The furnace temperature was adjusted slightly so as to maintain the reactor gas temperature at 1100 C. When all the flow parameters were stable, methane and acetylene were introduced according to the calculated flow rate for the particular SR2 in question. Instantly, the NOx output decreased and once it reached a steady value, the reading was recorded. A constant check on gas leaks was crucial to the success of the experiments. The procedure was repeated for various SR2 values (0.75-1.0) as well as for four reburn fuel combinations of methane and acetylene. As many as 20 runs were conducted to study the reburning effectiveness of methane/acetylene.

While the gas temperature 3" inside the reactor read 1100 C, the experiment was

performed for six SR2 values, namely, 0.75, 0.8, 0.85, 0.9, 0.95 and 1.0. The total flow rate of the gas mixture was 1950 cc/min. Given in Table 5.4 are the various flow rates of pure gases calculated for NO reburning with 90/10 fuel combination of methane and acetylene. Table 5.5 lists the actual flow rates, adjusted to accommodate varying gas proportions (that is, percent concentrations) in the cylinders such as oxygen/He, methane/He, acetylene/He and NO/He. These were calibrated for rotameter scales and fed through the respective flow meters. The steady readings on the NOx analyzer before addition of reburn fuel and after addition of reburn fuel were recorded. The experimental results for four combinations of methane/acetylene, namely, 95/5, 90/10, 85/15 and 80/20 are shown in Table 5.6. The results of NO reburning with 100% methane are also tabulated for the purpose of comparison.

Table 5.4 Simulated flow rates of various pure gases for NO reburning with 90/10 combination of methane/acetylene

SR2	CO_2	O_2	CH_4	C_2H_2	NO	He
0.75	313.5	36.0	75.9	8.4	1.95	1514.2
0.80	316.2	36.3	61.4	6.8	1.95	1527.3
0.85	318.6	36.6	48.4	5.4	1.95	1539.1
0.90	320.8	36.8	36.6	4.1	1.95	1549.7
0.95	322.8	37.1	26.0	2.9	1.95	1559.3
1.00	324.6	37.3	16.3	1.8	1.95	1568.1

Table 5.5 Adjusted flow rates accounting for gas proportions (% concentrations) in the cylinders for NO reburning with 90/10 combination of methane/acetylene

SR2	CO_2	O_2	CH_4	C_2H_2	NO	He
0.75	313.5	179.0	377.8	385.3	553.4	141.0
0.80	316.2	180.6	305.5	311.6	553.4	282.7
0.85	318.6	182.0	240.7	245.5	553.4	409.8
0.90	320.8	183.2	182.3	185.9	553.4	524.4
0.95	322.8	184.4	129.3	131.8	553.4	628.3
1.00	324.6	185.4	81.0	82.6	553.4	722.9

Table 5.6 Experimental results on NO reburning with various combinations of methane and acetylene

Gas Temperature 1100 C

SR2	100/0	95/5	90/10	85/15	80/20
0.75	-	1000/7	1000/8	-	-
0.8	1012/14	1000/7	1000/5	1000/5	1000/5
0.85	1018/10.3	1000/8	1000/6	1000/6	1000/6
0.9	1012/6	1000/8	1000/7	1000/4	1000/5
0.95	956/270	1000/453	1000/452	1000/410	1000/372
1.0	1018/852	1000/785	1000/753	-	-

NO in/out Concentrations are measured in ppm.

It can be seen from Table 5.6 that for the case of 100% methane as reburn fuel, NO reduction increases with increase in SR2 ratio until the optimum SR2 value of 0.9. The reduction is not as high for the cases of SR2 > 0.9. This behavior was documented in the previous report and it is consistent with the numerical predictions carried out earlier in the program.

For the case of 95% methane and 5% acetylene, a similar reduction is observed. The inlet concentration of NO (1000 ppm) reduces to mere single digits for the lower SR2 values (0.75-0.9), thus yielding a wider SR2 window that favors NO reduction. The reduction is 55% at SR2=0.95 and only 21% at SR2=1.0. Again, the experimental results of NO reduction with a combination of methane and acetylene follow the same trend predicted computationally.

It can be noticed also that NO reduction is almost the same for various methane/acetylene combinations. It means that a slight addition of acetylene is enough to strengthen the reductive effectiveness of methane. In effect, the addition of acetylene will enhance the operating window considerably from a narrow 0.85-0.9 SR2 range for methane to 0.75-0.9 SR2 range for all combinations of methane and acetylene.

5.1.3 Experimental results on NO reburning with methane/ ammonia

Presented here are the experimental results of NO reburning with methane/ammonia. The results are consistent with the computational work submitted in Chapter III. These experiments marked the completion of gaseous phase experiments under this study.

The experimental procedure employed for nitric oxide reburning with methane/ammonia was very similar to the one employed for reburning with methane/acetylene combination. First, the furnace was started and with its temperature set point control, a furnace temperature in the neighborhood of 1140 C was set. Slowly, helium, oxygen and carbon dioxide cylinders were opened and the flow levels calculated for a particular reburning stoichiometric ratio (SR2) were set. Oxygen simultaneously flowed through the NOx

analyzer. The analyzer was turned on and allowed to warm up. The parameters on the analyzer were checked until they reached the normal operating conditions. Then, the nitric oxide flow was adjusted to 1000 ppm which was expressed on the NOx analyzer digital readout. The Omega probe measured the gas temperature inside the reactor which was digitized on the thermometer readout. The furnace temperature was adjusted slightly so as to maintain the reactor gas temperature at 1100 C. When all the flow parameters were stable, methane and ammonia were introduced according to the calculated flow rate for the particular SR2 in question. Instantly, the NOx output decreased and once it reached a steady value, the reading was recorded. A constant check on gas leaks was crucial to the success of the experiments. The procedure was repeated for various SR2 values (0.8-1.0) as well as for two reburn fuel combinations of methane and ammonia (98/2 and 96/4). The model results (Chapter III) steered the choice of input conditions in this experimental study on the reburning effectiveness of methane/ammonia. While the gas temperature 3" inside the reactor was steady at 1100 C, the experiment was performed for five SR2 values, namely, 0.8, 0.85, 0.9, 0.95 and 1.0. The total flow rate of the gas mixture was 1950 cc/min. Given in Table 5.7 are the various flow rates of pure gases calculated for NO reburning with 98/2 fuel combination of methane and ammonia. Table 5.8 lists the actual flow rates, adjusted to accommodate varying gas proportions (that is, percent concentrations) in the cylinders such as oxygen/He, methane/He, ammonia/He and NO/He. These were calibrated for rotameter scales and fed through the respective flow meters. The steady readings on the NOx analyzer before addition of reburn fuel and after addition of reburn fuel were recorded. The experimental results for 98/2 combination of methane/ammonia, with introduction of methane

only, methane and ammonia together and ammonia only (by closing methane feed and increasing ammonia to the allowable maximum through the rotameters) are shown in Table 5.9. The flow rates of pure gases and the adjusted rates were calculated for the 96/4 combination of methane and ammonia and the entire cycle of experiments was performed at SR2 values of 0.85, 0.9, 0.95 and 1.0. The results of these experiments are presented in Table 5.10.

Table 5.7 Simulated flow rates of various pure gases for NO reburning with 98/2 combination of methane/ammonia

SR2	CO_2	O_2	CH_4	NH_3	NO	He
0.80	315.8	36.2	69.3	1.41	1.95	1525.3
0.85	318.3	36.5	54.6	1.11	1.95	1537.5
0.90	320.6	36.8	41.4	0.84	1.95	1548.5
0.95	322.6	37.0	29.3	0.60	1.95	1558.4
1.00	324.5	37.4	18.4	0.38	1.95	1567.5

Table 5.8 Adjusted flow rates accounting for gas proportions (% concentrations) in the cylinders for NO reburning with 98/2 combination of methane/ammonia

SR2	CO_2	O_2	CH_4	NH_3	NO	He
0.80	315.8	180.4	344.9	151.4	553.4	404.2
0.85	318.3	181.8	271.8	306.2	553.4	318.5
0.90	320.6	183.1	205.8	445.9	553.4	241.2
0.95	322.6	184.3	146.0	572.5	553.4	171.1
1.00	324.5	185.3	91.5	687.9	553.4	107.3

Table 5.9 Experimental results on NO reburning with reburn fuel of 98% methane and 2% ammonia

Gas Temperature 1100 C

SR2	NO in	NO_{out}* methane only	NO_{out} CH_4 and NH_3	NO_{out}* ammonia only
0.8	1020	43	**24**	885
0.85	1010	37	**24**	860
0.9	990	31	**22**	845
0.95	1022	310	**275**	934
1.0	1080	940	**905**	1045

NO in/out Concentrations are measured in ppm.
* Not representative of SR2 value. Based on cutting off one or the other reburn fuel from the reaction mixture.

Table 5.10 Experimental results on NO reburning with reburn fuel of 96% methane and 4% ammonia

Gas Temperature 1100 C

SR2	NO_{in}	NO_{out}* methane only	NO_{out} CH_4 and NH_3	NO_{out}* ammonia only
0.85	994	38	**34**	697
0.9	1012	32	**22**	789
0.95	1000	431	**352**	861
1.0	1014	928	**865**	929

NO in/out Concentrations are measured in ppm.
* Not representative of SR2 value. Based on cutting off one or the other reburn fuel from the reaction mixture.

It can be seen from Table 5.9 as well as Table 5.10 that for the case of methane only as reburn fuel, NO reduction increases with increase in SR2 ratio until the optimum SR2 value of 0.9. The reduction is not as high for the cases of SR2 > 0.9. This behavior was

documented in the previous report and is consistent with the numerical predictions carried out earlier in the program.

For the case of 98% methane and 2% ammonia (Table 5.9), a significant NO_x reduction is observed. The inlet concentration of NO (1000 ppm) reduces to lower twenties in the ppm level for the SR2 values upto 0.9. The reduction is 73% at SR2=0.95 and only 16.2% at SR2=1.0. These experimental results of NO reduction with a combination of methane and ammonia follow the same trend predicted computationally.

It can be noticed from Table 5.10 that NO reduction is similar (to the above trend) for 96/4 combination of methane/ammonia. The maximum reduction occurs at SR2=0.9. The reduction is less at higher SR2 ratios: 64.8% at 0.95 and only 14.7% at 1.0. However, comparing the levels with the introduction of methane only, it can be inferred that a slight addition of ammonia favors the NO_x reduction further by strengthening the reductive effectiveness of methane. It can be further observed from Tables 5.9 and 5.10 that the additional effect of ammonia on NO_x reduction is more pronounced at SR2 > 0.9 than SR2 < 0.9. This is due to the fact that the methane-NOx reaction is not close to the equilibrium in the former case (SR2 > 0.9) than the latter case.

Also shown in Tables 5.9 and 5.10 is the exit concentration of NO when methane feed was cut off and only ammonia was used as the reburn fuel. This was deliberately planned to see the performance of ammonia as a primary reburn fuel. The reduction of nitric oxide was not much, a maximum of 14.6% for 98/2 run and about 22% for 96/4 run. Thus it was concluded that the use of ammonia in small quantities is helpful in NO_x reduction chiefly as a reburn fuel additive to methane.

The above findings are significant in terms of the industry needs. With methane as a reburn fuel, the narrow operating window calls for precise cascade control between the primary zone combustion feed inlet, the reburning zone methane inlet and the NO_x analyzer in order that the NO_x emissions be within permissible limits. However, with the addition of acetylene or ammonia to methane as reburn fuel, the NO_x emissions will be within permissible limits as long as a set point control is given to the methane/acetylene or methane/ammonia reburning feed inlet not to exceed the SR2 of 0.9. With the latter case, the operation is easier to keep the NO_x emissions within limits even if there arise some changes in the primary zone combustion feed inlet.

5.2 Heterogeneous Reactions in NO_x Reduction

Several experiments were conducted to study heterogeneous combustion in the reactor with the use of the carefully designed coal feeder. These experiments included reburning with coal (several samples), char gasification, and surface catalysed reburning. The results are presented in the order just referred to.

5.2.1 Reburning with methane and coal

Conducting reburning experiments with coal was the most difficult part of our project as we faced persistent problems with the operation of the coal feeder. Some of the challenges have already been discussed in Chapter IV. These challenges gave us the impetus to stay focused and our efforts have been met with success as several coal samples were tested for their reburning effectiveness. Here are the results of those experiments.

5.2.1.1 Reburning studies with DECS-23 coal sample

The research team selected DECS-23, a high volatile A bituminous Pittsburgh coal (Washington county sample obtained in 1994) from the PennState Coal Sample Databank for the preliminary testing. As outlined in Chapter IV, the coal feeder assembly was incorporated in the experimental setup; and the experimental conditions for methane reburning were set. The nitric oxide level was set at 1000 ppm as in all the previous experiments. A continuous coal feeding was verified and the NO_x reduction was checked. No significant impact of the presence of coal was seen initially so long as the methane was not introduced. This indicated that coal is effective only under reducing conditions. Hence, methane was introduced without the feeding of the coal and the reduction was achieved. As expected from the knowledge of prior reburning experiments, the reduction was slight (6%) at SR2=1.0 and quite considerable (55%) at SR2=0.95. When coal was introduced (uniformly) along with methane, further reduction was observed: the reduction was very significant (98%) at SR2=0.95, although slight reduction (8%) was achieved at SR2=1.0 as well. Table 5.11 lists the NO_x readings for these tests.

Table 5.11. NO_x reading during reburning with methane and coal (DECS-23 sample), ppm

Initial NO_x set at 1000 ppm.

SR2	With methane only	With methane and coal
1.0	940	917
0.95	450	18

5.2.1.2 Reburning studies with DECS-24 coal sample

Having tried reburning with DECS-23, a high volatile A bituminous Pittsburgh coal earlier, the research team selected DECS-25 sample obtained from the PennState Coal Sample Databank for its reburning effectiveness. This sample is a Montana lignite coal (Richland county sample obtained in 1994). Several attempts were made to feed the coal into the reactor but they failed. It was then decided that the coal be mixed with silica gel and then introduced into the reactor in order to achieve free flow of the coal into the reactor. The research team shifted its attention on another coal sample while waiting on the silica gel, back ordered from Fisher Scientific.

A high volatile C bituminous coal (sample DECS-24, Illinois #6 Seam, Macoupin county) was tested in the coal feeder and found to flow uniformly as the feeding mechanism lowered the feeder. The coal feeder assembly was then incorporated in the experimental setup; and the experimental conditions for methane reburning were set. The nitric oxide level was set at 1000 ppm as in all the previous experiments. A continuous coal feeding was verified and the NO_x reduction was checked. No significant impact of the presence of coal was seen initially while methane was not introduced, very much like what we observed in the case of DECS-23. This reiterated our earlier observation that coal is effective only under reducing conditions. Suspending the feeding of the coal, methane was introduced and as expected, reduction was achieved. In line with the data obtained from prior reburning experiments, the reduction was 57% at SR2=0.95. When coal was introduced (uniformly) along with methane, further reduction was observed: the reduction was very significant (96%). Listed below are the NO_x readings on the analyzer read-out during reburning with

methane and DECS-24 coal sample.

Initial NO_x set at 1000 ppm.
SR2=0.95

With methane only: 430 ppm

With methane and coal: 39 ppm

It is apparent that the introduction of coal aids the reduction of NOx by reburning with methane at SR2=0.95 quite considerably. The level of reduction achieved by methane alone at SR2=0.9 (upto <50 ppm out of 1000 ppm) can now be obtained at SR2=0.95 with the introduction of coal, thereby initiating some heterogeneous reactions to boost NOx reduction.

5.2.1.3 Reburning studies with DECS-25 coal sample

The difficulty of feeding the DECS-25 coal sample (Montana lignite coal, Richland county), was solved by mixing the sample with silica gel, on a 50-50 weight basis. The coal bed did not get packed and the uniform feeding was achieved in this process. After ensuring the free flow of the coal-silica gel mixture, the coal feeder assembly was incorporated in the experiment and the experimental conditions for methane reburning were set. The nitric oxide level was set at 1000 ppm as in all the previous experiments. While methane was introduced (as per SR2=0.95 conditions), the NO_X reduced to 461 ppm. A continuous feeding of the coal-silica gel mixture was verified and further reduction was checked. The reduction was observed for two feed rates, referred to hereafter as Rate I (speed 5 on the variable speed motor of the coal feeding mechanism) and Rate II (speed 7 on the variable speed motor). The

feed rates presented below the table represent only the amount of coal fed per minute while the same amount of silica gel is also fed in that time. So the feed rate of the mixture is twice the feed rate of the coal. Table 5.12 lists NO_X readings on the analyzer read-out.

Table 5.12 NO_x reading during reburning with methane and coal (DECS-25 sample), ppm

Initial NOx set at 1000 ppm.

SR2	With methane only	With methane and coal
0.95	461	39[*] 16[+]

[*]Rate I: 0.114 gm/min of DECS-25 coal
[+]Rate II: 0.13 gm/min of DECS-25 coal

It is apparent that the introduction of coal aids the reduction of NO_X by reburning with methane at SR2=0.95 quite considerably. The level of reduction achieved by methane alone at SR2=0.9 (up to <50 ppm out of 1000 ppm) can now be obtained at SR2=0.95 with the introduction of coal. Addition of coal enhances NO_X reduction, as a result of coal char gasification.

5.2.2 Reburning studies with activated carbon

Having seen favorable NOx reduction with several coal samples, the research team felt the need to attempt reburning with activated carbon, as an appropriate closing point for coal reburning experiments. Since this is a pure carbon with less than 1% impurities, the best possible reduction was expected. The results were in line with the expectation. The activated carbon was the most freely flowing and hence, the easiest to feed, of all the samples tried.

Presented in Table 5.13 are the NO_X readings on the analyzer read-out.

Table 5.13 NO_X reading during reburning with methane and activated carbon, ppm

Initial NO_X set at 1000 ppm.

SR2	With methane only	With methane and activated carbon
0.95	447	7^* 7^+

*Rate I: 0.154 gm/min
+Rate II: 0.232 gm/min

As seen in the case of lignite coal, activated carbon reburning experiments confirmed significant NO_X reduction by char gasification. It can be concluded from the results presented above that the reduction achieved by activated carbon (upto 7 ppm) in aiding reburning with methane is very significant as a NO_X reduction strategy in industrial applications in order to meet environmental regulations. Increasing the amount of activated carbon (as shown by Rate II) did not matter once the reduction was achieved. It can be safely said that the presence of activated carbon boosts heterogeneous reactions with the gas mixture inside the reactor maintained at 1100 C. Modeling char gasification reactions in this setting would be a useful study for future.

5.2.3 Surface catalyzed reburning studies

An important phase under this grant instrument was to conduct surface catalyzed reburning studies as a potential alternative for NO_x control in industrial applications. In deliberation with the concerned project personnel at the Department of Energy, it was decided

that calcium sulfide and calcium carbide would be used to conduct reburning studies and estimate their catalytic effect on NO_X reduction under pulverized coal combustion conditions.

5.2.3.1 Study with calcium sulfide

Calcium sulfide, as obtained from Aldrich, is in powdered form and tends to pack very quickly. Obviously, it could not be fed properly into the reactor. A procedure similar to that used for the Montana lignite coal was employed. An equal amounts of CaS and silica gel were mixed together uniformly and the mixture was placed in the plexi-glass chamber of the feeder. The feeder and the feeding mechanism are the same as those used for feeding coal. Upon setting all the experimental conditions for reburning with methane at SR2=0.95 and achieving NO_X reduction from 1000 ppm to 453 ppm, the uniform feeding of the CaS- silica gel was maintained. Speed 9 on the variable speed motor was employed to allow for the maximum feed rate of 0.12 gm/min of CaS (or, 0.24 gm/min of CaS- silica gel mixture). With the calcium sulfide supply at the rate of 0.12 gm/min, NO_X reduced to 205 ppm, increasing the reduction from 55% to 80% overall. This reduction proves that CaS offers catalytic surface, thereby enhancing an additional 25% NO_X reduction. The observations are presented below.

NO_X exit concentration during reburning with methane and calcium sulfide:

Initial NO_X: 1000 ppm. SR2: 0.95. Reaction temperature: 1100 C.

With methane only: 453 ppm

With methane and calcium sulfide[@]: 205 ppm

[@] Feed Rate of CaS: 0.12 gm/min

5.2.3.2 Study with calcium carbide

Calcium carbide, unlike calcium sulfide, was received as 8 mm thick pieces and had to be ground to fine particles in order to be fed through the coal feeder. There was no problem of the bed being packed and the flow into the reactor was uniform. Calcium carbide was also purchased from Aldrich. Presented in Table 5.14 are the NO_X readings on the analyzer readout.

Table 5.14 NO_X exit concentration during reburning with methane and calcium carbide, ppm

Initial NO_X: 1000 ppm. Reaction Temperature: 1100 C.

SR2	With methane only	With methane and calcium carbide
0.95	467	152[*] 113[+]

[*]Rate I: 0.106 gm/min
[+]Rate II: 0.122 gm/min

The feed rate of 0.106 gm/min (Rate I) for calcium carbide shows a significant NO_X reduction, namely, 53% with methane alone and 85% with both methane and calcium carbide. The feed rate of 0.122 gm/min (Rate II) shows further reduction, up to 89%. This experiment further confirms our previous conclusion that calcium associated compound offers a catalytic surface thereby abetting NO_X reduction significantly. Since Rate II in this experiment is comparable to the feed rate of calcium sulfide that yielded reduction up to about 80%, it can be further concluded that calcium carbide seems to show higher catalytic effect

on NO_X reduction than calcium sulfide. Modeling these surface reactions would be a worthwhile study in future.

Presented in the next chapter are the conclusions and recommendations.

Chapter VI

CONCLUSIONS AND RECOMMENDATIONS

In this work, both computer simulation and experimental studies were conducted to investigate several strategies for NO_x reduction under pulverized coal combustion conditions with an aim to meet the stringent environmental standards for NO_x control. Both computer predictions and reburning experiments yielded favorable results in terms of NO_x control by reburning with a combination of methane and acetylene as well as non-selective catalytic reduction of NO with ammonia following reburning with methane. The greatest reduction was achieved at the reburning stoichiometric ratio of 0.9; the reduction was very significant, as clearly shown in Chapters III and V. Both the experimental and computational results favored mixing gases: methane and acetylene (90% and 10% respectively) and methane and ammonia (98% and 2%) in order to get optimum reduction levels which can not be achieved by individual gases at any amounts. Also, the above gaseous compositions as reburning fuels seemed to have a larger window of stoichiometric ratio (SR2 < 0.9) as opposed to just methane (SR2=0.9) so as to reduce and keep NO_x at low ppm levels. From the various computational runs, it has been observed that although there are several pathways that contribute to NO_x reduction, the key pathway is $NO \rightarrow HCN \rightarrow NH_3 \rightarrow N_2+H_2$. With the trends established in this work, it is possible to scale the experimental results to real time industrial applications using computational calculations.

Heterogeneous reactions were carried out by feeding several coal samples, activated carbon and calcium compounds, individually upon reburning with methane under SR2=0.95 conditions. We have found that activated carbon char gasification reduces NO_x significantly

in methane reburning conditions, equivalent to homogeneous gas reburning as experienced with methane and acetylene/ammonia. Also, reactions with coal, both bituminous and lignite, reduced NO_x to acceptable low levels, most reasonably due to char gasification as well as surface catalyzed reactions of trace elements/minerals in coal. The calcium associated compounds offer catalytic surface and hence enhance NO_x reduction but not to the extent of char gasification. However, in general, when coal is reburnt, the two reactions, that is, heterogeneous char gasification and surface catalyzed reaction, may occur simultaneously, thereby bringing about NO_x reduction to its maximum. Therefore, coal having more of calcium sulfide or calcium carbide is preferred to maximize NO_x reduction.

One of the things we could not perform due to budgetary constraints is the mass balance around the experimental apparatus. The major gases exiting other than NO in our experiments were N_2 , CO_2 , CO, HCN, and NH_3. The gases such as CO, CO_2 , CH_4 and O_2 could be analyzed by a Non-Destructive Infrared (NDIR) analyzer (Model 1200 Fisher 11-128-1). Ammonia could be analyzed by specific ion electrodes (Orion Model 9512 BN) Range (1-1000 ppm) and HCN could be analyzed by Orion Model 94-06 BN along with a double junction reference electrode and an ionic strength adjuster (Range: 1-1000 ppm). Both NH_3 and HCN measurement would require an output meter (simultaneous, dual output). It is recommended that mass balance be planned in future efforts. However, mass balance was performed in the computer simulation work.

Our study concerned with reducing NO in the reburning zone. An extension of this study could be modeling or experimental analysis to investigate what would happen in the burnout zone. Song et al (1982) have published the decomposition of HCN as a function of

furnace temperature. It is shown that HCN is highly unstable at high temperatures and its recovery is reported to be 30% for a residence time of 1s at 1100 C. Hence, the high HCN observed at lower stoichiometries could be overcome by the burnout zone. Investigation of the burnout zone itself would be another worthwhile study.

Computational work pertaining to heterogeneous combustion is still an open door for investigation. Limited published data is available and with the use of Sandia's SURFACE CHEMKIN and other such tools, efforts could be made to simulate the heterogeneous experiments we have conducted under this grant instrument.

PAPERS/PRESENTATIONS

The following is a list of various publications and conference presentations resulted directly out of this grant instrument. A few more publications are expected in due time.

1. “Surface Catalyzed Nox Reduction by Calcium Compounds under Methane Reburning Conditions”, S.K. Kumpaty and K. Subramanian, *International Conference on Organic Synthesis-12*,Int’l Union of Pure and Applied Chemistry, Venice, Italy, June 28-July 2, 1998.

2. “Computational Modeling of Nitric Oxide Reduction in Coal Combustion”, S.K. Kumpaty, K. Subramanian and T. L. Hodges, ACS, I&EC Division, *Computers in Engineering 1997*, Birmingham, AL, May 5-7, 1997.

3. "Experimental Studies on NO_x Reduction by Reburning with Methane, Methane and Acetylene, and Methane and Ammonia”, S.K. Kumpaty, T.L. Hodges, K. Subramanian and V.P. Nokku, *The Fifth Annual HBCU/PS/Fossil Energy Research and Development Technology Transfer Symposium*, Baton Rouge, LA, March 4-5, 1997.

4. "Effect of Acetylene and Ammonia as Reburn Fuel Additions to Methane in Nitric Oxide Reburning", S.K. Kumpaty, K. Subramanian and V.P. Nokku, *The Fourth Annual HBCU/PS/Fossil Energy Research and Development Technology Transfer Symposium*, Greensboro, NC, April 2-4, 1996.

5. "Nitric Oxide Reburning with Methane", S.K. Kumpaty and K. Subramanian, *The Fourth Annual HBCU/PS/Fossil Energy Research and Development Technology Transfer Symposium*, Greensboro, NC, April 2-4, 1996.

6. "Computational Results on NO_x Reduction by Reburning with Methane", S.K. Kumpaty and K. Subramanian, *The Third Annual HBCU/PS/Fossil Energy Research and Development Technology Transfer Symposium*, Atlanta, GA, April 27-29, 1995.

PERTINENT REFERENCES

Angelos Kokkinos, "Reburning for cyclone boiler retrofit NO_x control", Environmental Division Research Update, *EPRI Journal*, Dec 1992.

Arthur Levy, "Unresolved Problems in SO_x, NO_x, Soot Controls in Combustion", *Nineteenth Symposium (International) on Combustion*, The Combustion Institute, p. 1227, 1982.

Baulch, D.L. and et al. "Summary Table of Evaluated Kinetic Data for Combustion Modeling: Supplement 1", *Combustion and Flame*, Vol. 98, pp. 59-79, 1994.

Bose, A.C., K.M. Danneker, and J.O.L. Wendt, "Coal Composition Effects on Mechanism Governing the Destruction of NO and Other Nitrogenous Species during Fuel-Rich Combustion", *Energy and Fuels*, Vol. 2, p. 301, 1988.

Bowman, C.T, "Chemistry of Gaseous Pollutant Formation and Destruction", Fossil Fuel Combustion- A Source Book, Edited by Bartol, W. And A.F. Sarofim, pp. 215-260, 1991.

Byrne, G.D. and Dean, A.M., "The Numerical Solution of Some Kinetic Models with Vode and Chemkin II", *Computers Chem*., Vol. 17, pp. 297-302, 1993.

Burch, T.E., F.R. Tillman, W.Y. Chen, T.W. Lester, R.B. Conway, and A.M. Sterling, "Partitioning of Nitrogenous Species in the Fuel Rich Stage of Reburning", *Energy and Fuels*, Vol. 5(2), p. 231, 1991a.

Burch, T.E., R.B. Conway, and W.Y. Chen, "A Practical Pulverized Coal Feeder for Bench - Scale Combustion Requiring Low Feed Rates", *Rev. Sci. Instrum*., Vol. 62(2), p. 480, 1991b.

Chan, L.K., A.F. Sarofim, and J.M. Beer, "NO Carbon Reaction Kinetics", *Combustion Flame*, Vol. 52(37), p. 45, 1983.

Cowley, L.T., and P.T. Roberts, Paper presented at the Fluidized Combustion Conference, held at the Energy Research Institute, Univ. Of Capetown, South Africa, 28- 30th January, 1981.

Chen, S.L., M.P. Heap, D.W. Pershing, and G.B. Martin, "Fate of Coal Nitrogen during Combustion", *Fuel*, Vol. 61(12), p. 1218, 1982.

Chen, S.L., J.C. Kramlich, W.R. Seeker, and D.W. Perishing, "Optimization of reburning for advanced NO_x control on coal-fired boilers", *Journal of Air and Waste Management Association*, Vol. 39, pp. 1375-1379, 1989.

Clean Coal Technology Demonstration Program, Program Update 1991, U.S. Department of Energy, Washington, DC 20585.

Davidson, D.F., M.D. DiRosa, A.Y. Chang, and R.K. Hanson, *Eighteenth International Symposium on Shock Waves,* Springer Verlag, Vol. 2, p. 813, 1991.

De Soete, G.G., "Mechanisms of Nitric Oxide Reduction on Solid Particles", Fifth EPA Fundamental Combustion Research Workshop, p.174, Newport Beach, CA, January 23-25, 1980.

East, A.L.L. and W.D. Allen, *Journal of Chemical Physics*, Vol. 99, p. 4638, 1993.

Engel, G., "Formation of Hydrogen Cyanide by the Action of Nitrogen Oxide on Natural gas under Atmospheric Pressure , II. The influence of steam, Hydrogen and Oxygen", *Compt. Rend*., Vol. 231, p. 1493, 1950.

Fenimore, C.P., "Formation of Nitric Oxide in Premixed Hydrocarbon Flames", *Thirteenth Symposium (International) on Combustion*, The Combustion Institute, p. 373, 1971.

Freihaut, J.D. and D.J. Seery, "A Phenomemological Understanding and Model of Fuel Bound Nitrogen Release in Coal Devolatilization and Pyrolysis", *International Conference on Coal Science*, Sydney, Austraila, p. 957, October 1985.

Furasawa, T., D. Kunii, A. Oguma, and N. Yamada, "Rate of Reduction of Nitric Oxide by Char", *International Chemical Engineering*, Vol. 20(2), pp. 239-244, 1980.

Furasawa, T., M. Tsujimura, K. Yasunaga, and T. Kojima, "Fate of Fuel Bond Nitrogen within Fluidized Bed Combustor under Staged Air Firing", *Eighth (International) Fluidized Bed Combustion*, Vol. 3, p. 1095, 1985.

Furasawa, T., M. Tsunoda, and D. Kunii, "Nitric Oxide Reduction by Hydrogen and Carbon Monoxide over Char Surface", Chemical Reaction Engineering- Boston, *American Chemical Society* Symposium series #196, Vol. 29, pp. 347-357, 1982.

Glarborg, P. and et al., "A Flow Reactor Study of HNCO Oxidation Chemistry", *Combustion and Flame*, Vol. 98, pp. 241-258, 1994.

Glarborg, P. and J.A. Miller, "Mechanism and Modeling of Hydrogen Cyanide Oxidation in a Flow Reactor", *Combustion and Flame*, Vol.99, pp. 475-483, 1994.

Glarborg, P., J.E. Johnson, and K. Dam-Johnson, "Kinetics of Homogeneous Nitrous Oxide Decomposition", *Combustion and Flame*, Vol. 99, pp. 523-532, 1994.

Greene, G.C., and R.E.C. Weaver., Proceedings of the Joint VTG-AIChE Meeting, Munchen BRD, Vol. 4, pp. 5-11, September 1974.

Haider, G., Micronized Coal Testing (Phase 1), Alliance Research Center Report 5277, Babcock and Wilcox, Alliance, Ohio, 1982.

Hansen, P.F.B., K. Dam-Johansen, J.E. Johnsson, and T. Hulgaard, "Catalytic Reduction of NO and N_2O on Limestone during Sulfur Capture under Fluidized Bed Combustion Conditions", *Chemical Engineering Science*, Vol. 47(9-11), pp. 2419-2424, 1992.

Helble, J.J., S. Srinivasachar, and A.A. Boni, "Factors Influencing the Transformation of Minerals During Pulverized Coal Combustion", *Prog. Energy Combustion Science*., Vol. 16, p. 267, 1990.

Huffman, G.P., F.E. Huggins, N. Shah and A. Shah, "Behavior of Basic Elements During Coal Combustion", *Prog. Energy Combustion Science*., Vol. 16, pp. 243-251, 1990.

Kee, R.J., F.M. Rupley, and J.A. Miller, "Chemkin- II: A Fortran Chemical Kinetics Package for the Analysis of Gas Phase Chemical Kinetics", Sandia Report No. SAND 89-8009B, April 1994.

Kilpinen, P., P. Glarborg, and M. Hupa, "Reburning Chemistry: A Kinetic Modeling Study", *Ind. Eng. Chem. Res*., Vol. 31, pp. 1477-1490, 1992.

Kumpaty, S.K., "Simulation of Coal and Char Nitrogen Reactions in Combustion", Final Technical Report, *U.S. Department of Energy (PETC)*, Grant No. DE-FG22-92MT92022, October 1993.

Lee, S-D. and S-H. Chung, "On the Structure and Extinction of Interacting Lean Methane/Air Premixed flames", *Combustion and Flame*, Vol. 98, pp. 80-92, 1994.

Levy, J.M., L.K. Chan, A.F. Sarofim, and J.M. Beer, "NO/Char reactions at Pulverized Coal Flame Conditions", *Eighteenth (International) Symposium on Combustion*, The Combustion Institute, pp. 111-120, 1981.

Lindstedt, R.P., F.C. Lockwood, and M.A. Selim, "Detailed Kinetic Modeling of Chemistry and Temperature effects on Ammonia Oxidation", *Combustion Science and Technology*, Vol. 99, pp. 253-276, 1994.

Lutz, A.E., R.J. Kee, and J.A. Miller, "SENKIN: A Fortran Program for Predicting Homogenous Gas Phase Chemical Kinetics with Sensitivity Analysis", Sandia Report SAND87-8248.UC4, February, 1988; May 1994.

Miller, J.A., and C.T. Bowman, "Mechanism and Modelling of Nitrogen Chemistry in Combustion", *Prog. Energy Combust. Science*, Vol. 15(4), p. 287, 1989.

Miller, J.A. and C.T. Bowman, *International Journal of Chemical Kinetics,* Vol. 23, p. 289, 1991.

Miller, J.A. and C.F. Melius, *International Journal of Chemical Kinetics,* Vol. 24, p. 421, 1992.

Miller, J.A., and G.A. Fisk, "Combustion chemistry", Special Report, *Chemical and Engineering News,* August 31, 1987.

Mulholland, J.A., and W.S. Lanier., "Application of Reburning for NO_x Control to a Firetube Package Boiler", EPA-600/D-84-170, US EPA, June, 1984.

Mulholland, J.A., and R.E. Hall, Proceedings of the 1985 Symposium- Stationary Combustion NO_x Control , 1, Utility Boiler Application, EPRI CS-4360, Jan., 1986

Overmoe, B.J., J.M. McCarthy, S.L. Chen, W.R. Seeker, G.D. Silcox, and D.W. Pershing., Proceedings of the 1985 Symposium- Stationary Combustion NO_x Control, 1, Utility boiler application, EPRI CS-4360, Jan., 1986.

Patry, M., and G. Engel, "Formation of Hydrocyanic acid by the action of Nitric Oxide on Methane at Atmospheric Pressure I. General Conditions of formation," *Compt. Rend.*, Vol. 231, p. 1302, 1950.

Perishing, D.W., M.P. Heap, W.R. Seeker, "Bench-Scale Studies to Identify Process Parameters Controlling Reburning with Pulverized Coal", EPA Project Summary, EPA/600/S7-89/005, 1990.

Seeker, W.R., "The kinetics of ignition and particle burnout of coal dust suspensions under rapid heating conditions", Ph.D. Dissertation, Kansas State University, 1979.

Singoredjo, L., F. Kapteijn, J.A. Moulijn, and H.P. Boehm, "Modified Activated Carbons for the Selective Catalytic Reduction of NO with NH_3", *Carbon*, Vol. 31(1), pp. 213-222, 1993.

Song, Y.H., J.H. Pohl, J.M. Beer and A.F. Sarofim, "Nitric Oxide Formation During Pulverized Coal Combustion", *Combustion Science and Technology*, Vol. 28, pp. 31-39, 1982.

Takahashi, Y., et al., Proc. 1982 Joint Symposium- Stationary Combustion NO_x Control, 1, EPRI Report NO CS-3182, July 1983.

Teng, H., E.M. Suuberg, and J.M. Calo, "Studies on the Reduction of Nitric Oxide by Carbon: The NO-Carbon Gasification reaction", *Energy and Fuels*, Vol. 6(4), p. 398, 1992.

Tsang, W., *Phys. Chem. Ref. Data*, Vol. 21, p. 753, 1992.

Tsang, W., and Herron, *Phys. Chem. Ref. Data*, Vol. 20, p. 609, 1991.

Tsujimura, M., T. Furasawa, and D. Kunii, "Catalytic Reduction of Nitric Oxide by Carbon Monoxide over Calcined Limestone", *Journal of Chemical Engineering of Japan*, Vol. 16(2), p. 132, 1983.

Vandooren, J., J. Bian, and P.J. Tiggelen, "Comparison of Experimental and Calculated Structures of an NH_3-NO Flame. Importance of the NH_2 + NO Reaction", *Combustion and Flame*, Vol. 98, pp. 402-410, 1994.

Vince.A., *The Clean Air Advisor*, Vol. 1(2), September 1992.

Wendt, J.O.L., C.V. Sternling, and M.A. Matrovich, *Fourteenth Symposium (International) on Combustion*, The Combustion Institute, p. 897, 1973.